The Boundary-Hopf-Fold Bifurcation in Filippov Systems*

Konstantinos Efstathiou†, Xia Liu‡, and Henk W. Broer†

Abstract. This paper studies the codimension-3 *boundary-Hopf-fold* (BHF) bifurcation of planar Filippov systems. Filippov systems consist of at least one *discontinuity boundary* locally separating the phase space to disjoint components with different dynamics. Such systems find applications in several fields, for example, mechanical and electrical engineering, and ecology. The BHF bifurcation appears in a subclass of Filippov systems that we call *Hopf-transversal* systems. In such systems an equilibrium of one vector field goes through a Hopf bifurcation while the other vector field is transversal to the boundary. Depending on the slope of the transversal vector field, different bifurcation scenarios take place. The BHF bifurcation occurs at a critical value of the slope that separates these scenarios. We derive a local normal form for the BHF bifurcation and show the eight different associated bifurcation diagrams. The local 3-parameter normal form topologically models the simplest way to generically unfold the BHF bifurcation. The BHF bifurcation is then studied in a particular example from population dynamics.

1. Introduction. *Filippov systems*, introduced in [18], are discontinuous dynamical systems composed of two or more smooth vector fields that are separated by discontinuity boundaries; the formal definition is given in section 2.1. For a thorough theoretical introduction to Filippov systems, we refer the reader to [15, 18, 26]. Such systems appear in applications such as control systems with switching control laws [1, 9, 12, 30, 31, 32], or population dynamics [11, 13, 20, 24]. See also [3, 17, 33] for more examples in these directions. Apart from these, Filippov systems also model mechanical systems exhibiting dry friction [2, 19, 21, 23, 25].

In this paper we focus on *Hopf-transversal* (HT) Filippov systems. Such systems consist of two smooth vector fields that are separated by a smooth discontinuity boundary. The vector field on one side undergoes a supercritical or subcritical Hopf bifurcation, while the vector field on the other side intersects the boundary transversally.

The Hopf bifurcation appears frequently in applications. For smooth dynamical systems a mature theory exists that discusses the Hopf bifurcation, but this theory cannot be directly

†Johann Bernoulli Institute for Mathematics and Computer Science, University of Groningen, Groningen, 9700 AK, The Netherlands (K.Efstathiou@rug.nl, H.W.Broer@rug.nl).

‡Corresponding author. School of Mathematics and Science, Shijiazhuang University of Economics, Shijiazhuang, 050031, People's Republic of China, and Johann Bernoulli Institute for Mathematics and Computer Science, University of Groningen, Groningen, 9700 AK, The Netherlands (liuxia1228@126.com). This author's research was supported by the NWO project "Stability, Bifurcations and Stabilisation of Invariant Sets in Differential Inclusions."

(a) boundary-Hopf   (b) boundary-fold
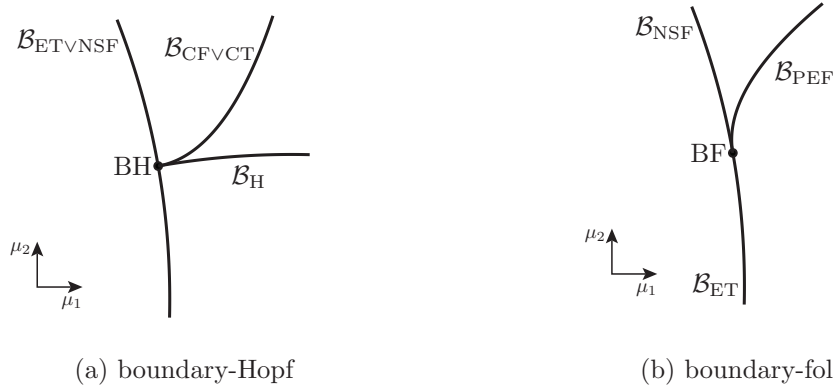
Figure 1. *Sketches of bifurcation diagrams for codimension-2 bifurcations. Here we assume that the system depends on two parameters, μ_1 and μ_2. For higher-dimensional parameter spaces these figures represent a two-dimensional cross-section of the parameter space. (a) Sketch of a boundary-Hopf (BH) bifurcation where a Hopf bifurcation, a grazing bifurcation, and an equilibrium transition (ET) or nonsmooth fold (NSF) bifurcation meet. The grazing bifurcation can either be a cycle transition (CT) or a cycle fold (CF). Compare to the four cases in Figure* 5. *(b) Sketch of a boundary-fold (BF) bifurcation where an equilibrium transition (ET), an NSF bifurcation, and a pseudoequilibria fold (PEF) bifurcation meet. Compare to cases* A1 *and* A2 *in Figure* 5.

generalized to discontinuous systems. In smooth vector fields, the Hopf bifurcation is determined by a pair of complex eigenvalues passing through the imaginary axis. However, the analysis of the Hopf bifurcation in the smooth context is not generally applicable to discontinuous vector fields due to the lack of a continuous linearization at the equilibrium when this lies on the boundary. It is therefore necessary to perform a corresponding analysis for the Hopf bifurcation in the Filippov setting.

Bifurcations where the discontinuity of the Filippov system plays an essential role (we talk here about discontinuity-induced bifurcations) appear, for example, in models of prey-predator ecosystems subject to on-off harvesting control [11, 14, 24]. Accordingly, there has been considerable work focusing on this type of bifurcation; see [10, 11, 16, 22].

In the context of HT systems, [11] considers the unfolding of the codimension-2 *boundary-Hopf* (BH) bifurcation where an equilibrium of one smooth vector field goes through a Hopf bifurcation while it lies on the boundary. In the BH bifurcation, the codimension-1 Hopf bifurcation of the equilibrium is accompanied by a subordinate codimension-1 grazing bifurcation of limit cycles; see Figure 1(a). A suitable nondegeneracy condition ensures that the same equilibrium simultaneously goes through a discontinuity-induced bifurcation that is either an *equilibrium transition* or a *nonsmooth fold*; see section 2.2.1 for precise definitions and for the form of the nondegeneracy condition. Furthermore, these discontinuity-induced bifurcations form another codimension-1 family of bifurcations; see Figure 1(a).

A bifurcation scenario complementary to the BH bifurcation is when a *hyperbolic* equilibrium (i.e., not undergoing a Hopf bifurcation) is transversally crossing the boundary while the previously mentioned nondegeneracy condition fails. This scenario gives a *boundary-fold* (BF) bifurcation [8]. The bifurcation diagram of the BF bifurcation is presented in Figure 1(b). The codimension-2 BF bifurcation occurs at the boundary in parameter space between two codimension-1 bifurcations, equilibrium transition and nonsmooth fold. Furthermore, the BF

Type	Bifurcation set
Hopf	$\mathcal{B}_{\mathrm{H}}$
Equilibrium transition	$\mathcal{B}_{\mathrm{ET}}$
Nonsmooth fold	$\mathcal{B}_{\mathrm{NSF}}$
Pseudoequilibria fold	$\mathcal{B}_{\mathrm{PEF}}$
Cycle transition	$\mathcal{B}_{\mathrm{CT}}$
Cycle fold	$\mathcal{B}_{\mathrm{CF}}$

bifurcation is accompanied by a subordinate fold bifurcation of pseudoequilibria; see Figure 1(b).

Considering now the codimension-2 BH and BF bifurcations in a higher-dimensional parameter space, such as a 3-parameter family, we expect that there will exist parameter values where these bifurcations coincide. We call such parameter values *boundary-Hopf-fold* (BHF) bifurcation points.

The BHF point acts as the organizing center for the families of codimension-1 and -2 bifurcations appearing in its neighborhood. This can already be seen in simpler situations, such as with two saddle-node curves meeting at a cusp point. In another context, codimension-3 bifurcations have been shown to act as organizing centers in a predator-prey model with nonmonotonic response [6]. In our particular case, studying the full neighborhood of the BHF point is essential for anticipating and understanding the bifurcation diagrams that appear in applications. For example, in the context of the predator-prey model studied in section 6, if one focuses at the BH point, then it becomes easy to miss the nearby family of pseudoequilibria fold (PEF) bifurcations (see Figure 10(c)) since it is not predicted by the *local* analysis of the BH bifurcation. Nevertheless, knowing that the BH bifurcation is close enough to a BHF bifurcation, and knowing the unfolding of the latter, allows us to anticipate the existence of the PEF family and to efficiently locate it in the bifurcation diagram.

Our aim is to *describe the generic unfoldings of the BHF bifurcation* which then include all the 5 codimension-1 bifurcation families associated to the BH and BF bifurcations and listed in Table 1. Thus a direct study of a neighborhood of BHF points is required in order to obtain the local bifurcation diagram, to understand how all the codimension-1 and -2 bifurcations interact, and to obtain a model that is stable under perturbations.

As we shall see in section 3 the BHF unfolding has codimension 3. We show that the coalescence of the BH and BF bifurcations accounts for all the bifurcations observed in the neighborhood of BHF bifurcation points. From this point of view the current work can be considered as an extension of [10, 22]. Furthermore, our analysis reveals that in order to obtain a stable model it is not enough to consider a transversal vector field that is constant; we must also consider nontrivial linear terms.

The inspiration for this work has been the work by Di Bernardo, Pagano, and Ponce [16], where a 2-parameter family of HT systems with a BHF bifurcation was considered. The bifurcation diagram for this family is presented in Figure 2. Observe that all the codimension-1 bifurcations associated to the BH and the BF coalesce in this system at the BHF point.
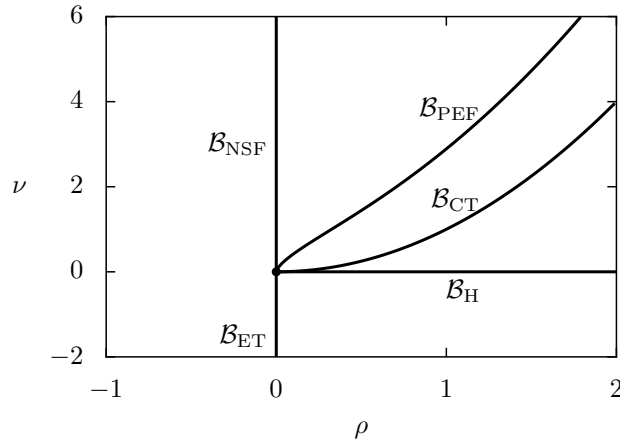
Figure 2. *Bifurcation diagram of the 2-parameter family studied in [16]. Five codimension-1 bifurcations meet at the origin. For the labeling of the codimension-1 bifurcations we refer the reader to Table 1. Note that the tangency of $\mathcal{B}_{\mathrm{PEF}}$ and $\mathcal{B}_{\mathrm{NSF}}$ is of order 3/2. In particular, the origin corresponds to a degenerate BHF bifurcation that does not satisfy the requirements of Definition 3.1.*

However, the model of [16] is not generic in the sense that an arbitrarily small perturbation of the system qualitatively changes the bifurcation diagram by splitting the BH and BF points. This behavior reflects the fact that the BHF bifurcation has codimension 3. The reason for the nongeneric character of the system studied in [16] is that the vector field at one side of the discontinuity boundary was chosen to be perpendicular to the boundary. The analysis in the present work clearly demonstrates the reason for the nongenericity and furthermore shows how to modify the nongeneric model in order to obtain a generic 3-parameter family with persistent dynamics: allow the slope of the transversal vector field to change while adding nontrivial linear terms to it.

We briefly outline the structure of this paper. In the next section we give an overview of Filippov dynamics and introduce different types of equivalence between Filippov systems. In section 3 we construct formal normal forms for the HT system. Subsequently, in section 4 we compute the universal bifurcation diagram of the HT system. After that, we investigate the dynamics of the truncated formal normal forms in section 5. In section 6 we study a model from population dynamics, show that it goes through a BHF bifurcation, and determine its type. Finally, in section 7 we summarize the main results and point out further research directions.

2. Preliminaries. In this section we give the definition of Filippov systems and describe their dynamical properties and bifurcations that are important for our purposes in this paper. Furthermore, we review different types of equivalence between Filippov systems.

2.1. Definition of Filippov dynamics. A Filippov system Z defined on a two-dimensional manifold M is a triplet (X, Y, f). Here X and Y are $\mathcal{C}^r$ ($r \geq 1$ or $r = \infty$) vector fields and are extendable over a full neighborhood of the boundary Σ. The latter is given as the zero-set of the $\mathcal{C}^r$ function $f : M \to \mathbb{R}$, that is,

$$\Sigma = \{(x, y) \in M : f(x, y) = 0\}.$$

We assume that 0 is a regular value of f, and thus Σ is a smooth one-dimensional submanifold of M. Note that if we are interested only in local behavior near a certain point (x_0, y_0) of Σ, we can replace the previous global smoothness condition with the requirement that (x_0, y_0) be a regular point of f, i.e., $\nabla f(x_0, y_0) \neq 0$, so that Σ is *locally* a smooth one-dimensional manifold.

The discontinuity boundary Σ separates the open subsets M_X and M_Y of M, defined as

$$M_X = \{(x,y) \in M : f(x,y) < 0\} \quad \text{and} \quad M_Y = \{(x,y) \in M : f(x,y) > 0\}.$$

The dynamics of Z in M_X and M_Y are defined by the flows of X and Y, respectively. This means that for $(x,y) \in M \setminus \Sigma$, Z is given by

$$(2.1) \qquad Z(x,y) = \begin{cases} X(x,y) & \text{for } (x,y) \in M_X, \\ Y(x,y) & \text{for } (x,y) \in M_Y. \end{cases}$$

Meanwhile, on Σ, Filippov's convex method [18] prescribes two types of dynamics. In order to give a formal description of these two types, the boundary Σ is divided into the *crossing set*

$$(2.2a) \qquad \Sigma_c = \{(x,y) \in \Sigma : \mathcal{L}_X f(x,y) \, \mathcal{L}_Y f(x,y) > 0\}$$

and the *sliding set*

$$(2.2b) \qquad \Sigma_s = \{(x,y) \in \Sigma : \mathcal{L}_X f(x,y) \, \mathcal{L}_Y f(x,y) \leq 0\},$$

where $\mathcal{L}_X f(x,y)$ denotes the Lie (or directional) derivative of f with respect to the vector field X at the point (x,y), that is, $\mathcal{L}_X f = (X \cdot \nabla) f$. Note that $\Sigma = \Sigma_s \cup \Sigma_c$.

It follows from (2.2) that if at a point $(x,y) \in \Sigma$ the vector field X points toward Σ and Y points away from Σ, or vice versa, then $(x,y) \in \Sigma_c$. In the former case, where X points toward and Y points away from Σ, an orbit of Z that arrives at (x,y) following the flow of X continues from (x,y) following the flow of Y. Thus the orbit is a continuous, but in general nonsmooth, curve that crosses from M_X to M_Y. If Y points toward Σ while X points away, then the orbit crosses, in the same way, from M_Y to M_X. For concreteness, for $(x,y) \in \Sigma_c$ we specify that $Z(x,y) = X(x,y)$ if X points toward Σ and that $Z(x,y) = Y(x,y)$ in the opposite case.

If, on the other hand, at a point $(x,y) \in \Sigma$ both vector fields point toward Σ or away from Σ, then $(x,y) \in \Sigma_s$. In this case, the dynamics at (x,y) are defined by the vector $Z_s(x,y)$ which is the unique convex linear combination of $X(x,y)$ and $Y(x,y)$ that is tangent to Σ at (x,y). Therefore, an orbit starting at $(x,y) \in \Sigma_s$ moves along the boundary. Specifically, the *sliding vector field* Z_s is defined by Filippov [18] as

$$(2.3) \qquad Z_s(x,y) = \frac{\mathcal{L}_X f(x,y) \, Y(x,y) - \mathcal{L}_Y f(x,y) \, X(x,y)}{\mathcal{L}_X f(x,y) - \mathcal{L}_Y f(x,y)},$$

provided that $\mathcal{L}_X f(x,y) \neq \mathcal{L}_Y f(x,y)$. It can be verified, using (2.3), that $\mathcal{L}_{Z_s} f(x,y) = 0$, i.e., $Z_s(x,y)$ is tangent to Σ at (x,y). In the case where $\mathcal{L}_X f(x,y) = \mathcal{L}_Y f(x,y)$ for $(x,y) \in \Sigma_s$ (further implying $\mathcal{L}_X f(x,y) = \mathcal{L}_Y f(x,y) = 0$) we then define $Z(x,y) = 0$.

Summarizing, for $(x, y) \in \Sigma$, we define Z as

$$(2.4) \qquad Z(x, y) = \begin{cases} Z_s(x, y) & \text{for } (x, y) \in \Sigma_s, \text{ where } \mathcal{L}_X f(x, y) \neq \mathcal{L}_Y f(x, y), \\ 0 & \text{for } (x, y) \in \Sigma_s, \text{ where } \mathcal{L}_X f(x, y) = \mathcal{L}_Y f(x, y) = 0, \\ X(x, y) & \text{for } (x, y) \in \Sigma_c, \text{ where } \mathcal{L}_X f(x, y) < 0, \\ Y(x, y) & \text{for } (x, y) \in \Sigma_c, \text{ where } \mathcal{L}_X f(x, y) > 0. \end{cases}$$

Points $(x, y) \in \Sigma_s$, where $\mathcal{L}_X f(x, y) = 0$ (resp., $\mathcal{L}_Y f(x, y) = 0$), are called *tangency points* of X (resp., Y). Generically, the function $\mathcal{L}_X f(x, y) \mathcal{L}_Y f(x, y)$ changes sign at a tangency point, and therefore such points are generically positioned at the boundary of the sliding set Σ_s.

2.2. Bifurcations in Filippov systems. We now give a brief description of the main organizing centers of the dynamics, such as equilibria and limit cycles, appearing in two-dimensional Filippov systems, and of their bifurcations. We focus on those structures that are specific to Filippov systems and appear in our HT family.

The equilibria of X in M_X and of Y in M_Y are also equilibria of Z. Equilibria of X or Y in Σ are called *boundary equilibria*. Note that if $(x, y) \in \Sigma$ is an equilibrium of either X or Y (but not of both), then $(x, y) \in \Sigma_s$ and $Z_s(x, y) = 0$.

Finally, equilibria of X in M_Y and of Y in M_X will be called *virtual equilibria*. Note that virtual equilibria do not affect the dynamics of Z but that introducing the concept facilitates the description of bifurcations in Filippov systems where an equilibrium crosses the discontinuity boundary.

A point $(x, y) \in \Sigma_s$ is called a *pseudoequilibrium* of Z if $Z_s(x, y) = 0$. Geometrically, a pseudoequilibrium occurs when the vector fields X and Y are transversal to Σ and anti-collinear. Note that one can use (2.3) to extend the sliding vector field Z_s to all points in $\Sigma \setminus \{(x, y) : \mathcal{L}_X f(x, y) = \mathcal{L}_Y f(x, y)\}$. Note that outside Σ_s, the extended vector field Z_s is no longer a convex linear combination of X and Y. If $Z_s(x, y) = 0$ for some (x, y) in the crossing region Σ_c, then we call such point a *virtual pseudoequilibrium* of Z.

A *sliding cycle* is a closed orbit of Z that is composed of an orbit segment of Z_s on the sliding set Σ_s and an orbit segment of one of the smooth vector fields, either X or Y, in M_X or M_Y, respectively; see the leftmost frame in Figure 4(a).

2.2.1. Equilibrium transition and nonsmooth fold bifurcation. When an equilibrium of Z collides with the discontinuity boundary we generically have either an *equilibrium transition* (ET) or a *nonsmooth fold* (NSF) bifurcation; cf. [15, 16]. In the ET the equilibrium collides with a virtual pseudoequilibrium and they give their place to a virtual equilibrium and a pseudoequilibrium; see Figure 3(a). In the NSF bifurcation the equilibrium collides with a pseudoequilibrium and they both become virtual; see Figure 3(b).

The following theorem, proved in [15], gives conditions for the occurrence of an ET or NSF bifurcation in a Filippov system $Z = (X, Y, f)$ that smoothly depends on a parameter β. Here $X = X(x, y; \beta)$ and $Y = Y(x, y; \beta)$ are smooth vector fields, and the discontinuity boundary is a smooth curve given by $\Sigma = \{(x, y) : f(x, y; \beta) = 0\}$ with f a smooth function.

Theorem 2.1 (ET and NSF bifurcation [15]). *Assume that $X(0, 0, 0) = 0$ and $D_{(x,y)} X(0, 0, 0)$ is nonsingular. Moreover, assume that for $\beta = 0$ an equilibrium branch $(x(\beta), y(\beta))$ of the*

(a) ET bifurcation   (b) NSF bifurcation
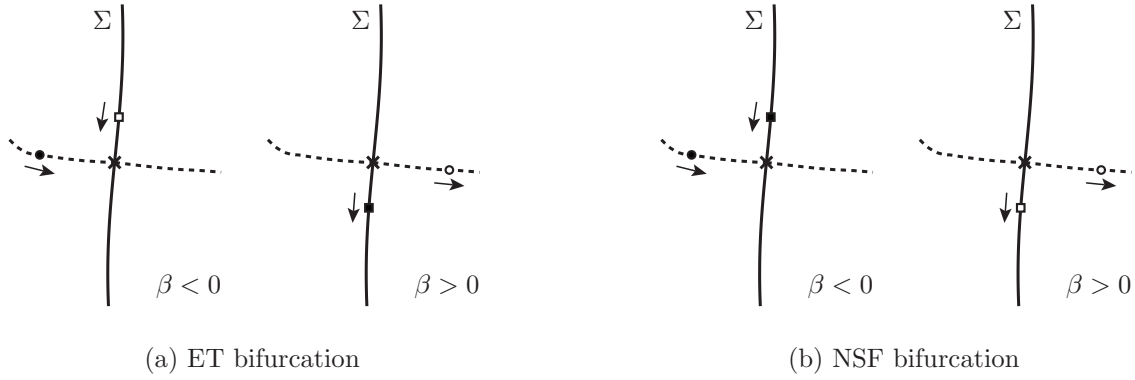
Figure 3. *ET and NSF bifurcations. The discontinuity boundary Σ is displayed as a solid line. The dashed line represents the motion of the equilibrium of one of the vector fields as a parameter changes. Round points represent equilibria (filled) or virtual equilibria (hollow). Squares represent pseudoequilibria (filled) or virtual pseudoequilibria (hollow). The cross marks where the equilibrium and the pseudoequilibrium meet when $\beta = 0$.*

vector field $X(x, y, \beta)$ transversally crosses the discontinuity manifold Σ at $(x, y, \beta) = (0, 0, 0)$, that is,

$$\left. \frac{d}{d\beta} \right|_{\beta=0} f(x(\beta), y(\beta), \beta) \neq 0.$$

Finally, assume that the nondegeneracy condition

$$\delta := D_{(x,y)} f(0, 0, 0)(D_{(x,y)} X(0, 0, 0))^{-1} Y(0, 0, 0) \neq 0$$

is satisfied. Then, at $\beta = 0$, there is an ET if $\delta > 0$ and an NSF if $\delta < 0$.

2.2.2. Grazing bifurcations of limit cycles: Cycle transitions and cycle folds. A grazing bifurcation occurs when the limit cycle of X touches the boundary Σ. Depending on the stability type of the smooth limit cycle from inside, two generic cases are associated with the grazing bifurcation; cf. [24]. The first case is called *cycle transition*: the limit cycle touches Σ at a point and becomes a sliding cycle; see Figure 4(a). In this case the limit cycle is stable from inside. In the second case, called *cycle fold*, an unstable limit cycle and a stable sliding cycle initially coexist. When the limit cycle touches Σ it collides with the sliding cycle; more precisely, the two cycles coincide. After the collision both cycles disappear; see Figure 4(b).

2.3. Equivalence between Filippov systems. An important part of this study is the classification of Filippov systems up to some kind of equivalence. In the literature several such kinds of equivalence have been proposed. We discuss here those used in the present work.

The simplest type of equivalence between Filippov systems is *smooth equivalence*; cf. [22].

Definition 2.2 (smooth equivalence). *Two Filippov systems $Z = (X, Y, f)$ and $\tilde{Z} = (\tilde{X}, \tilde{Y}, \tilde{f})$ are smoothly equivalent if there exist a diffeomorphism $\varphi : \mathbb{R}^2 \to \mathbb{R}^2$ in phase space, strictly positive smooth functions $K_X : \mathbb{R}^2 \to \mathbb{R}$, $K_Y : \mathbb{R}^2 \to \mathbb{R}$, and a strictly increasing smooth function $k : \mathbb{R} \to \mathbb{R}$ with $k(0) = 0$ such that*

(2.5) $D\varphi \cdot X = (K_X \tilde{X}) \circ \varphi, \quad D\varphi \cdot Y = (K_Y \tilde{Y}) \circ \varphi, \quad f = k \circ \tilde{f} \circ \varphi.$
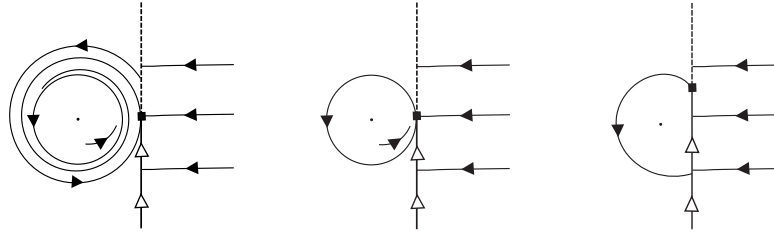
(a) Cycle transition. A limit cycle touches the boundary and becomes a grazing cycle.
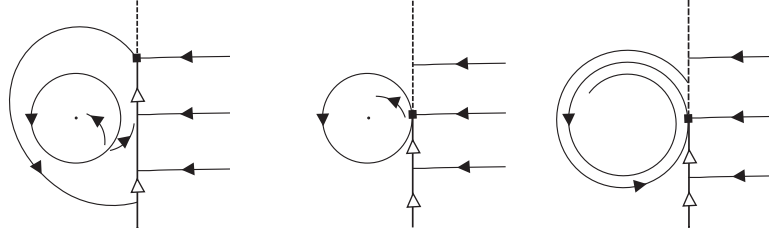
(b) Cycle fold. A limit cycle and a grazing cycle collide and disappear.

Figure 4. *Two cases of grazing bifurcation; cf.* [24]. *The discontinuity boundary Σ is represented by the vertical line; Σ_s is the solid part and Σ_c the dashed part. The hollow arrows in Σ_s show the direction of the flow of Z_s. The boundary between Σ_s and Σ_c is the tangency point represented by the black square.*

Note that the functions K_X and K_Y in Definition 2.2 induce time rescalings of the vector fields $\tilde{X}$ and $\tilde{Y}$, respectively. Furthermore, $\tilde{f}$ and $k \circ \tilde{f}$ have the same zero level set and thus define the same boundary.

3. Normal form for the boundary-Hopf-fold bifurcation. In this section we first define the boundary-Hopf-fold (BHF) bifurcation and then derive a formal normal form for it. We study the bifurcation diagram in section 4.

Definition 3.1 (BHF bifurcation). *Consider a general planar Filippov system $Z = (X, Y, f)$ smoothly depending on parameters $\mu \in \mathbb{R}^m$, $m \geq 3$, and such that there exists a μ-dependent family of points $(x_0(\mu), y_0(\mu)) \in \mathbb{R}^2$ with $X(x_0, y_0; \mu) = 0$ for all μ. Denote by $\alpha(\mu) \pm i\omega(\mu)$ the eigenvalues of the linearization $D_{(x,y)}X(x_0, y_0; \mu)$ and by $\ell_1(\mu)$ the first Lyapunov coefficient of X at (x_0, y_0) (see [28, 29] or (3.3) below for the definition of ℓ_1). Furthermore, let*

$$\delta(\mu) = \nabla_{(x,y)} f(x_0, y_0; \mu)(D_{(x,y)}X(x_0, y_0; \mu))^{-1} Y(x_0, y_0; \mu).$$

We say that the system goes through a BHF *bifurcation at $\mu = \mu_0$ when the following conditions are satisfied:*

(i) $f(x_0, y_0; \mu_0) = 0$, $\nabla_{(x,y)} f(x_0, y_0; \mu_0) \neq 0$, and $\nabla_\mu g(\mu_0) \neq 0$, where $g(\mu) = f(x_0, y_0; \mu)$.

(ii) $\alpha(\mu_0) = 0$, $\omega(\mu_0) > 0$, $\ell_1(\mu_0) \neq 0$, and $\nabla_\mu \alpha(\mu_0) \neq 0$.

(iii) $\mathcal{L}_Y f(x_0, y_0; \mu_0) \neq 0$; that is, $Y(x_0, y_0; \mu_0)$ is transversal to Σ_{μ_0} at (x_0, y_0).

(iv) $\delta(\mu_0) = 0$ with $\nabla_\mu \delta(\mu_0) \neq 0$.

(v) $\nabla_\mu g(\mu_0)$, $\nabla_\mu \alpha(\mu_0)$, and $\nabla_\mu \delta(\mu_0)$ are linearly independent.

Condition (i) in Definition 3.1 says that at $\mu = \mu_0$ the equilibrium (x_0, y_0) of X transversally crosses the discontinuity boundary Σ_{μ_0}; the latter is *locally* a smooth one-dimensional

submanifold of $\mathbb{R}^2$. Condition (ii) implies that, at the same parameter value $\mu = \mu_0$, the vector field X goes through a Hopf bifurcation.

Recall also that when the point (x_0, y_0), which is an equilibrium for X, meets the boundary it generically goes through either an NSF bifurcation or an ET; cf. Theorem 2.1. The type of bifurcation depends on the sign of δ: for $\delta < 0$ the system goes through an NSF bifurcation; for $\delta > 0$ it goes through an ET. Condition (iv) in Definition 3.1 implies that at $\mu = \mu_0$, where $\delta = 0$, the situation is degenerate.

Theorem 3.2 (formal normal form). *Consider a BHF bifurcation point μ_0 of a Filippov system Z; see Definition 3.1. Then at (x_0, y_0) there is a local diffeomorphism φ that depends smoothly on parameters μ and a smooth invertible reparameterization $\mu \mapsto \lambda = (\rho, \nu, \gamma, \lambda_4, \ldots, \lambda_m)$ such that the original Filippov system is smoothly equivalent, in the sense of Definition 2.2, to the system*

$$(3.1\mathrm{a}) \qquad Z(x, y; \lambda) = \begin{cases} X(x, y; \lambda) & \text{for } f(x, y; \lambda) < 0, \\ Y(x, y; \lambda) & \text{for } f(x, y; \lambda) > 0, \end{cases}$$

with

$$(3.1\mathrm{b}) \qquad X(x, y; \lambda) = \begin{pmatrix} \nu & -1 \\ 1 & \nu \end{pmatrix} \begin{pmatrix} x \\ y \end{pmatrix} + \kappa(x^2 + y^2) \begin{pmatrix} x \\ y \end{pmatrix} + O((x, y)^4; \lambda),$$

$$(3.1\mathrm{c}) \qquad Y(x, y; \lambda) = \begin{pmatrix} \sigma \\ \gamma - \sigma\nu + a_1(\lambda)x + a_2(\lambda)y + O((x, y)^2; \lambda) \end{pmatrix},$$

and

$$(3.1\mathrm{d}) \qquad f(x, y; \lambda) = x - \rho + O((x, y)^2; \lambda),$$

where $\kappa = \operatorname{sgn}(\ell_1(\mu_0)) = \pm 1$ and $\sigma = \operatorname{sgn}(\mathcal{L}_Y f(x_0, y_0; \mu_0)) = \pm 1$. All higher order terms in X, Y, and f smoothly depend on λ.

The parameters ρ, ν, γ that appear in the normal form (3.1) have the following interpretations. First, ρ determines the passage of the equilibrium of X through the boundary Σ which occurs at $\rho = 0$. Then, X goes through a Hopf bifurcation at $\nu = 0$. Finally, γ determines whether we have an ET or an NSF bifurcation when the equilibrium of X crosses Σ; the two cases are separated by $\gamma = 0$.

3.1. Proof of Theorem 3.2. We construct the formal normal form (3.1) in successive steps.

Step 1. A μ-dependent translation brings the equilibrium (x_0, y_0) of X_μ to the origin $(0, 0) \in \mathbb{R}^2$.

Step 2. Since $\nabla_\mu g(\mu_0)$, $\nabla_\mu \alpha(\mu_0)$, and $\nabla_\mu \delta(\mu_0)$ are linearly independent, there is a smooth invertible parameterization $\mu \mapsto \lambda = (\tilde\rho, \tilde\nu, \tilde\gamma; \lambda_4, \ldots, \lambda_m)$ in an open neighborhood of μ_0 in parameter space such that in the new parameters we have $g(\lambda) = -\tilde\rho$, $\alpha(\lambda) = \tilde\nu$, and $\delta(\lambda) = \tilde\gamma$. Furthermore, we choose the reparameterization so that μ_0 maps to $\lambda_0 = 0 \in \mathbb{R}^m$.

Step 3. Let $h(x, y; \lambda) = f(x, y; \lambda) + \tilde\rho$. Since $\nabla_{(x,y)} h(x_0, y_0; \lambda_0) = \nabla_{(x,y)} f(x_0, y_0; \lambda_0) \neq 0$, we can define a smooth λ-dependent coordinate transformation so that in the new coordinates, that we still denote by (x, y), we have $h(x, y; \lambda) = x$. Then, in these coordinates we have $f(x, y; \lambda) = x - \tilde\rho$.

Step 4. Note that the eigenvalues of $D_{(x,y)}X(x_0, y_0; \lambda)$ in the new parameters are $\alpha(\lambda) \pm i\omega(\lambda) = \tilde{\nu} \pm i\omega(\lambda)$. The next step is to apply a linear coordinate transformation $T(\lambda)$, depending smoothly on λ, in order to transform X to

$$X(x, y; \lambda) = \begin{pmatrix} \tilde{\nu} & -\omega(\lambda) \\ \omega(\lambda) & \tilde{\nu} \end{pmatrix} \begin{pmatrix} x \\ y \end{pmatrix} + O((x,y)^2; \lambda).$$

Note that the linear part of X is invariant under rotations and uniform coordinate scalings. This means that we can choose the linear transformation $T(\lambda)$ so that it has the form

$$T(\lambda) = \begin{pmatrix} 1 & 0 \\ T_1(\lambda) & T_2(\lambda) \end{pmatrix}.$$

The benefit of such a choice is that it leaves invariant the function $f(x, y; \lambda) = x - \tilde{\rho}$.

Note, furthermore, that smooth invertible coordinate transformations leave invariant the value of δ. This implies that in the new coordinates we have that

$$\nabla_{(x,y)}f(0, 0; \lambda)(D_{(x,y)}X(0, 0; \lambda))^{-1}Y(0, 0; \lambda) = \tilde{\gamma}.$$

Computing the left-hand side of the last relation gives

(3.2)
$$\frac{\tilde{\nu}Y_1(0, 0; \lambda) + \omega(\lambda)Y_2(0, 0; \lambda)}{\tilde{\nu}^2 + \omega(\lambda)^2} = \tilde{\gamma}.$$

Therefore, for $\lambda = 0$ (which implies $\tilde{\nu} = \tilde{\gamma} = 0$ and $\omega(\lambda) \neq 0$) we find that $Y_2(0, 0; 0) = 0$. Furthermore, from the assumption that Y is transversal to the discontinuity boundary at the origin we find that $Y_1(0, 0; 0) \neq 0$.

Step 5. A smooth, λ-dependent, near-identity coordinate transformation containing only quadratic and higher order terms in x, y (cf. [4, 5]) brings the vector field X to the form

$$X(x, y; \lambda) = \begin{pmatrix} \tilde{\nu} & -\omega(\lambda) \\ \omega(\lambda) & \tilde{\nu} \end{pmatrix} \begin{pmatrix} x \\ y \end{pmatrix} + (x^2 + y^2) \begin{pmatrix} c(\lambda) & -d(\lambda) \\ d(\lambda) & c(\lambda) \end{pmatrix} \begin{pmatrix} x \\ y \end{pmatrix} + O((x,y)^4; \lambda).$$

Note that after this transformation the boundary Σ is deformed and is, in general, no longer a straight line. In particular, the function f in the new coordinates takes the form $f(x, y; \lambda) = x - \tilde{\rho} + O((x,y)^2; \lambda)$. It follows that $f(0, 0; \lambda) = -\tilde{\rho}$, and thus for $\tilde{\rho} = 0$ the boundary Σ contains the origin while the tangent vector to Σ at the origin is vertical.

Furthermore, note that since such a coordinate transformation does not contain linear terms, it does not affect the constant part of the vector field Y.

Step 6. Dividing X by the positive function $\varphi(x, y)$ given by

$$\varphi(x, y) = \omega(\lambda) + d(\lambda)(x^2 + y^2),$$

that is, by reparameterizing time, brings the last system to the form

$$X(x, y; \lambda) = \begin{pmatrix} \nu & -1 \\ 1 & \nu \end{pmatrix} \begin{pmatrix} x \\ y \end{pmatrix} + \ell_1(\lambda)(x^2 + y^2) \begin{pmatrix} x \\ y \end{pmatrix} + O((x,y)^4; \lambda).$$

Here

(3.3)
$$\ell_1(\lambda) = \frac{c(\lambda) - \nu d(\lambda)}{\omega(\lambda)}$$

is the first Lyapunov coefficient of X and $\nu = \tilde{\nu}/\omega(\lambda)$. Note that $d\nu/d\tilde{\nu}(0) = 1/\omega(0) \neq 0$, that is, the map $\tilde{\nu} \mapsto \nu$ is a smooth, locally invertible reparameterization. Therefore we can use the new parameter ν in place of $\tilde{\nu}$.

Step 7. Uniformly scaling the coordinates by $|\ell_1(\lambda)|^{1/2}$ can further simplify the system so that

$$X(x, y; \lambda) = \begin{pmatrix} \nu & -1 \\ 1 & \nu \end{pmatrix} \begin{pmatrix} x \\ y \end{pmatrix} + \kappa(x^2 + y^2) \begin{pmatrix} x \\ y \end{pmatrix} + O((x, y)^4; \lambda),$$

where $\kappa = \mathrm{sgn}(\ell_1(\lambda)) = \pm 1$. This step depends on the nondegeneracy conditions imposed on X(cf. [28, 29]), i.e., that the first Lyapunov coefficient $\ell_1(\lambda)$ is not zero. Since $\ell_1(0) \neq 0$, this scaling depends smoothly on λ.

Furthermore, after the scaling transformation, by also multiplying f by $|\ell_1(\lambda)|^{1/2}$ the boundary Σ can be expressed as the zero level set of the scaled function $f(x, y) = x - \rho + O((x, y)^2; \lambda)$, where $\rho = |\ell_1(\lambda)|^{1/2}\tilde{\rho}$.

Step 8. The previous uniform coordinate scaling changes the constant terms of Y to

$$Y(x, y; \lambda) = \begin{pmatrix} |\ell_1(\lambda)|^{1/2}Y_1(0, 0; \lambda) \\ |\ell_1(\lambda)|^{1/2}Y_2(0, 0; \lambda) \end{pmatrix} + O(x, y; \lambda).$$

We now rescale time for the flow of Y by dividing Y by its first component $\tilde{Y}_1(x, y; \lambda) = |\ell_1(\lambda)|^{1/2}|Y_1(0, 0; \lambda)| + O(x, y; \lambda)$. Note that $\tilde{Y}_1(0, 0; 0) = |\ell_1(0)|^{1/2}|Y_1(0, 0; 0)| \neq 0$; therefore there is a neighborhood of the origin in the product of phase space and parameter space where such rescaling is possible. Then we obtain

$$Y(x, y; \lambda) = \begin{pmatrix} \sigma \\ Y_2(0, 0; \lambda)/|Y_1(0, 0; \lambda)| \end{pmatrix} + \begin{pmatrix} 0 & 0 \\ a_1(\lambda) & a_2(\lambda) \end{pmatrix} \begin{pmatrix} x \\ y \end{pmatrix} + \begin{pmatrix} 0 \\ O((x, y)^2; \lambda) \end{pmatrix},$$

where $\sigma = \mathrm{sgn}(Y_1(0, 0; 0)) = \mathrm{sgn}(\tilde{Y}_1(0, 0; 0)) = \pm 1$. Also note that $\sigma = \mathrm{sgn}(\mathcal{L}_Y f(x_0, y_0; \mu_0))$ since it represents whether the flow of Y goes toward Σ or away from it and our coordinate transformations do not change this. Equation (3.2) can be rewritten as

$$\nu\sigma + \frac{Y_2(0, 0; \lambda)}{|Y_1(0, 0; \lambda)|} = \frac{\omega(\lambda)(\nu^2 + 1)}{|Y_1(0, 0; \lambda)|} \tilde{\gamma}.$$

Define a new parameter

$$\gamma = \frac{\omega(\lambda)(\nu^2 + 1)}{|Y_1(0, 0; \lambda)|} \tilde{\gamma},$$

and note that this induces a local diffeomorphism in parameter space. Then we can write Y in its final form as

$$Y(x, y; \lambda) = \begin{pmatrix} \sigma \\ \gamma - \sigma\nu + a_1(\lambda)x + a_2(\lambda)y + O((x, y)^2; \lambda) \end{pmatrix}.$$

This concludes the proof of Theorem 3.2.

4. Bifurcation diagram. In this section we show that the normal form (3.1) has five families of codimension-1 bifurcations. We describe in detail these families and how they fit together in the parameter space. We first consider the Hopf bifurcation and the grazing bifurcation which involve only the vector field X and the boundary. Then we consider together the ET and NSF bifurcations. Finally, we study the fold bifurcation of pseudoequilibria.

In order to state the main result we first introduce an extra bit of notation. Recall that in the normal form (3.1) the vector field Y becomes

$$Y(x, y; \lambda) = \begin{pmatrix} \sigma \\ \gamma - \sigma\nu + a_1(\lambda)x + a_2(\lambda)y + O((x, y)^2; \lambda) \end{pmatrix}.$$

Define the quantity

$$\xi(\lambda) = 2a_2(\lambda) - \sigma(1 + \nu^2)\frac{\partial^2 f}{\partial y^2}(0, 0; \lambda).$$

We will assume that ξ has a definite sign τ in the parameter region of interest, i.e., in a small enough neighborhood of the origin in parameter space. This can be ensured by checking that $\xi(0) \neq 0$. We show in the proof of Lemma 4.2 that this implies that the (one-dimensional) sliding vector field has a sign-definite quadratic part when it goes through a fold bifurcation, and therefore the fold bifurcation is nondegenerate. Under these assumptions we define $\tau = \operatorname{sgn} \xi(0)$. We can now state the following result.

Theorem 4.1 (HT bifurcation set). *There is an open neighborhood of the origin in the product of phase space (x, y) and parameter space (ρ, ν, γ), in which the HT formal normal form (3.1) has the following bifurcations:*

(i) *A codimension-2 boundary-Hopf (BH) bifurcation takes place at $\{\rho = 0, \nu = 0\}$. The BH bifurcation acts as the organizing center for the Hopf bifurcation and the grazing bifurcation. The Hopf bifurcation takes place on the set $\mathcal{B}_H = \{\rho \geq 0, \nu = 0\}$ and is supercritical for $\kappa = -1$ and subcritical for $\kappa = 1$. The grazing bifurcation is a cycle transition for $\kappa\sigma = 1$ while it is a cycle fold for $\kappa\sigma = -1$. It takes place on the set*

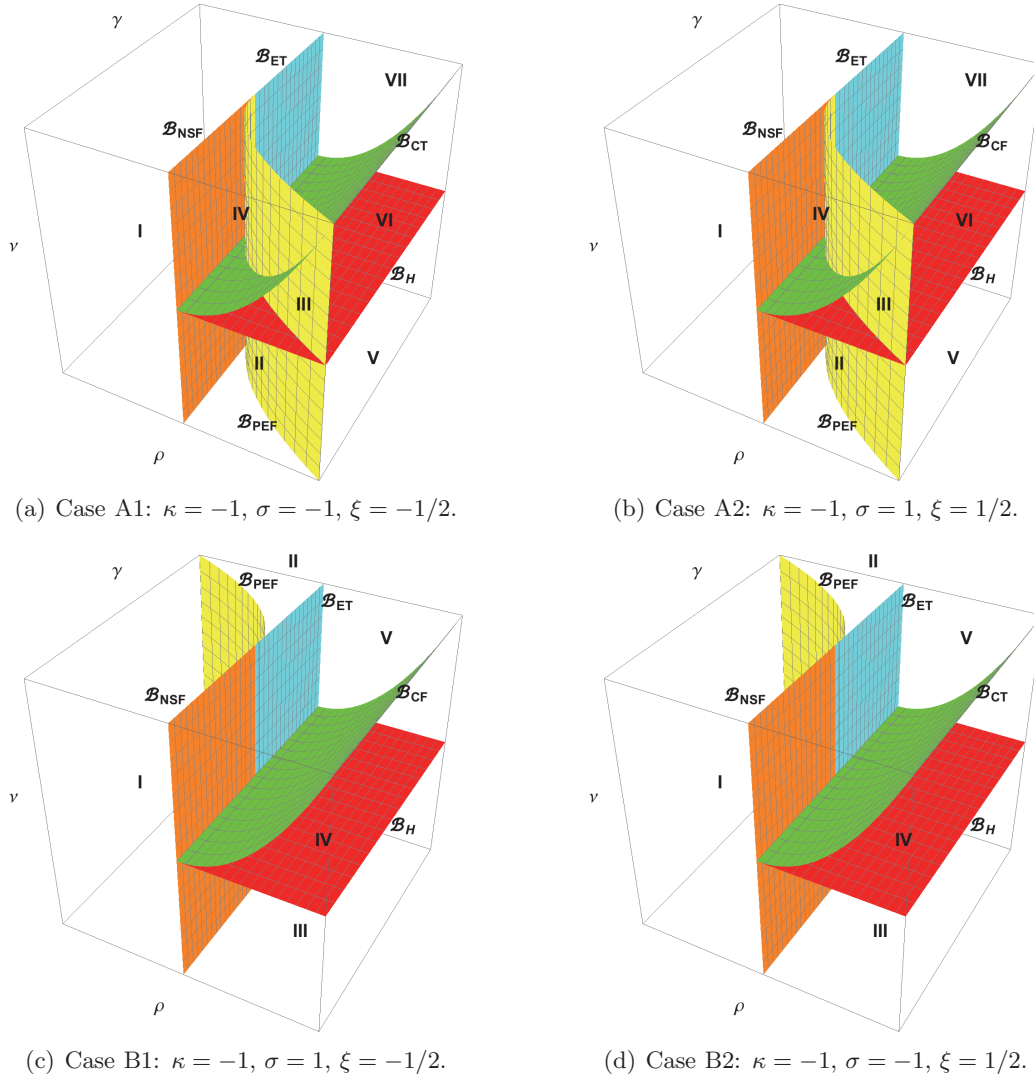$$\mathcal{B}_G = \{\nu = -\kappa\rho^2 + O(\rho^3), \rho \geq 0\}.$$

Furthermore, we denote the set $\mathcal{B}_G$ by $\mathcal{B}_{CT}$ when we have a cycle transition and by $\mathcal{B}_{CF}$ when we have a cycle fold.

(ii) *A codimension-2 boundary-fold (BF) bifurcation takes place at $\{\rho = 0, \gamma = 0\}$. The BF bifurcation acts as the organizing center for the ET, NSF, and pseudoequilibria fold (PEF) bifurcations. The ET takes place on the set $\mathcal{B}_{ET} = \{\rho = 0, \gamma > 0\}$ while the NSF takes place on the set $\mathcal{B}_{NSF} = \{\rho = 0, \gamma < 0\}$. Provided that $\xi(0) \neq 0$ the PEF bifurcation takes place on the set*

$$\mathcal{B}_{PEF} = \left\{\rho = \frac{1}{2\sigma\xi^0(\nu, \bar{\lambda})}\frac{\gamma^2}{1 + \nu^2} + O(\gamma^3), (\sigma\tau)\gamma \leq 0\right\},$$

where $\xi^0(\nu, \bar{\lambda}) = \xi(\rho = 0, \nu, \gamma = 0, \lambda_4, \ldots, \lambda_m)$.

Note that Theorem 4.1 describes eight different bifurcation diagrams depending on the values of $\kappa = \pm 1$, $\sigma\tau = \pm 1$, and $\kappa\sigma = \pm 1$, where $\tau = \operatorname{sgn}(\xi)$. Moreover, note that neglecting

(a) Case A1: $\kappa = -1$, $\sigma = -1$, $\xi = -1/2$.

(b) Case A2: $\kappa = -1$, $\sigma = 1$, $\xi = 1/2$.

(c) Case B1: $\kappa = -1$, $\sigma = 1$, $\xi = -1/2$.

(d) Case B2: $\kappa = -1$, $\sigma = -1$, $\xi = 1/2$.

Figure 5. *Bifurcation diagrams for the system Z_0 (5.1) in (ρ, ν, γ) space. Note that the grazing bifurcation for systems in the same row is of a different type: for $\kappa\sigma = 1$ (cases A1, B2) the limit and sliding cycles of Z_0 undergo a cycle transition while for $\kappa\sigma = -1$ (cases A2, B1) they undergo a cycle fold.*

higher order terms the bifurcation diagram is invariant under the discrete transformation $\mathcal{R} : (\kappa, \sigma, \xi; \rho, \nu, \mu) \mapsto (-\kappa, -\sigma, -\xi; \rho, -\nu, \mu)$. It is thus possible to fix $\kappa = -1$ and consider the four cases determined by the values of $\tau = \pm 1$ and $\sigma = \pm 1$. In Figure 5 we depict these four bifurcation diagrams in (ρ, ν, μ) space. As we show in section 5, the discrete transformation $\mathcal{R}$ can be amended by the mapping $(x, y, t) \mapsto (x, -y, -t)$ in phase space in order to provide a diffeomorphism between truncated normal forms. Therefore, the Filippov systems Z and $\mathcal{R}'Z$ have the same number of equilibria, pseudoequilibria, limit and sliding cycles, etc., but with opposite stability characteristics.

4.1. Proof of Theorem 4.1. We prove Theorem 4.1 by successively treating the codimension-1 bifurcations (Hopf, grazing, ET, NSF, and PEF).

Hopf bifurcation. In Theorem 3.2 we transformed the vector field X to the standard normal form for the Hopf bifurcation. Therefore, in the transformed system, the origin is an equilibrium of X and it goes through a Hopf bifurcation (supercritical or subcritical depending on κ) at $\nu = 0$. Nevertheless, the origin is an equilibrium of Z only when $\rho \geq 0$ (since for $\rho < 0$ the origin becomes a virtual equilibrium), and this accordingly restricts the set $\mathcal{B}_{\mathrm{H}}$.

Grazing bifurcation. The vector field X has a limit cycle only when $\kappa\nu \leq 0$ (without taking into account the discontinuity boundary). If we now also consider the effect of the boundary, we find that the limit cycle can go through a grazing bifurcation only when the equilibrium of X is real (as opposed to virtual). This implies that the grazing bifurcation can occur only in the region $\{\rho \geq 0, \kappa\nu \leq 0\}$ of the parameter space. To lowest order, the limit cycle touches the boundary when $\nu = -\kappa\rho^2$. Taking into account the higher order terms gives that the grazing bifurcation occurs at

$$\nu_G = -\kappa\rho^2 + O(\rho^3);$$

see [11] for details.

The exact type of grazing bifurcation (cycle transition or cycle fold) depends on the values of κ and σ. When $\kappa = -1$ (i.e., the Hopf bifurcation is supercritical) the generated, stable, limit cycle exists for $\nu \in (0, \nu_G)$. If, now, $\sigma = -1$, then at ν_G we have a cycle transition and for $\nu > \nu_G$ the limit cycle becomes a sliding cycle. If, on the other hand, $\sigma = 1$, then for $\nu < \nu_G$ the limit cycle coexists with a sliding cycle and at $\nu = \nu_G$ these cycles collide and disappear. For $\kappa = 1$ (i.e., when the Hopf bifurcation is subcritical) the generated, unstable, limit cycle exists for $\nu \in (\nu_G, 0)$. If $\sigma = -1$, then the limit cycle coexists with a sliding cycle for $\nu \in (\nu_G, 0)$. At ν_G these cycles collide, and for $\nu < \nu_G$ there are no cycles. Finally, if $\sigma = 1$, then for $\nu \in (\nu_G, 0)$ the system has only a limit cycle and for $\nu < \nu_G$ it has a sliding cycle.

ET and NSF bifurcation. In particular, for the formal normal form (3.1) we find that the origin transversally meets Σ at $\rho = 0$ and it can go either through an ET or an NSF bifurcation depending on the sign of

$$\delta(\lambda) := \nabla_{(x,y)} f(0, 0; \lambda)(D_{(x,y)} X(0, 0; \lambda))^{-1} Y(0, 0; \lambda) = \frac{\gamma}{1 + \nu^2};$$

see Theorem 2.1. This implies that the plane $\rho = 0$ is a bifurcation set and is separated by the line $\gamma = 0$ into two subsets containing ET and NSF bifurcations. In particular, for $\gamma > 0$ the origin goes through an ET while for $\gamma < 0$ through an NSF.

PEF bifurcation. The bifurcation sets $\mathcal{B}_{\mathrm{ET}}$ and $\mathcal{B}_{\mathrm{NSF}}$ meet along the line $\mathcal{B}_{\mathrm{BF}} = \{\rho = 0, \gamma = 0\}$ which is the set of BF bifurcations. The BF bifurcation is generically accompanied by a subordinate PEF bifurcation [8]. We now study in more detail the latter bifurcation and prove the following result.

Lemma 4.2 (PEF bifurcation). *Let $\xi \neq 0$. Then the normal form system* (3.1) *goes through a PEF bifurcation on the surface $\mathcal{B}_{\mathrm{PEF}}$ in the parameter space (ρ, ν, γ) parameterized as*

$$(4.1) \qquad \rho = \frac{1}{2\sigma\xi^0(\nu, \bar{\lambda})} \frac{\gamma^2}{1 + \nu^2} + O(\gamma^3), \quad \sigma\tau\gamma \leq 0,$$

where higher order terms in γ are also smooth functions of $\nu, \lambda_4, \ldots, \lambda_m$.

Proof. Recall that $(x_0, y_0) \in \Sigma$ is a pseudoequilibrium of Z if and only if it is an equilibrium of the sliding vector field Z_s, that is,

$$Z_s(x_0, y_0; \lambda) = 0.$$

Since $\nabla_{(x,y)} f(0,0) = (1,0)$, the boundary Σ can be locally parameterized by y. Thus for $(x,y) \in \Sigma$ we have $x = \rho + h(y; \lambda)$, where h is of second order in ρ and y. Therefore, pseudoequilibria (x_0, y_0) of Z are determined as roots y_0 of the equation

$$Z_s(\rho + h(y; \lambda), y; \lambda) = 0,$$

which depends only on y. Recall that the sliding vector field, Z_s, is tangent to Σ, and Σ is vertical at the origin. Therefore in order for y_0 to satisfy the last equation it is enough that it satisfies that $\zeta(y_0; \lambda) = 0$, where

$$\zeta(y; \lambda) := (Z_s)_2(\rho + h(y; \lambda), y; \lambda) = 0,$$

and $(Z_s)_2$ denotes the vertical component of Z_s.

We first prove that the conditions for the PEF bifurcation are satisfied at the origin. Below, for a function $q(y; \lambda)$ in the product of phase space and parameter space we will denote by q^0 the value of q at the point $y = 0$, $\rho = \gamma = 0$. Furthermore, we denote by q_y, q_ρ, etc., the partial derivative of q with respect to y, ρ, etc. We compute that

$$\zeta^0 = \zeta_y^0 = 0$$

and

$$\zeta_{yy}^0 = 2a_2^0 + (1 + \nu^2)\sigma h_{yy}^0 = 2a_2^0 - (1 + \nu^2)\sigma f_{yy}^0 = \xi^0 \neq 0,$$

where we use that $f(\rho + h(y, \lambda), y, \lambda) = 0$ implies $f_{yy}^0 = -h_{yy}^0$.

The common solution set of the equations $\zeta(y, \lambda) = 0$ and $\zeta_y(y, \lambda) = 0$ defines in the space $(y; \lambda)$ the fold bifurcation set $\mathcal{F}$ which projects in parameter space to the set $\mathcal{B}_{\mathrm{PEF}}$. Using the implicit function theorem we find that $\mathcal{F}$ is a codimension-2 manifold that goes through the origin, and is parameterized by $(\nu, \gamma, \lambda_4, \ldots, \lambda_m)$, since

$$\det \begin{pmatrix} \zeta_y^0 & \zeta_\rho^0 \\ \zeta_{yy}^0 & \zeta_{y\rho}^0 \end{pmatrix} = -\zeta_\rho^0 \zeta_{yy}^0 = -\sigma(1 + \nu^2)\xi^0 \neq 0,$$

where we have computed that $\zeta_\rho^0 = \sigma(1 + \nu^2)$ and $\zeta_{y\rho}^0 = a_1^0 - \nu a_2^0$. Thus in a neighborhood of $\{\rho = 0, \gamma = 0\}$ there exist smooth functions $\Psi(\nu, \gamma, \bar{\lambda})$, $R(\nu, \gamma, \bar{\lambda})$ such that

$$\zeta(\Psi(\nu, \gamma, \bar{\lambda}), R(\nu, \gamma, \bar{\lambda}); \lambda) = \zeta_y(\Psi(\nu, \gamma, \bar{\lambda}), R(\nu, \gamma, \bar{\lambda}); \lambda) = 0,$$

where $\bar{\lambda} = (\lambda_4, \ldots, \lambda_m)$.

We then compute that $\Psi_\gamma^0 = -1/\xi$, $R_\gamma^0 = 0$, $R_{\gamma\gamma}^0 = \sigma[\xi(1 + \nu^2)]^{-1}$. Thus $\mathcal{B}_{\mathrm{PEF}}$ can be locally expressed as

$$\rho = R(\nu, \gamma, \bar{\lambda}) = \frac{1}{2\sigma\xi^0} \frac{\gamma^2}{1 + \nu^2} + O(\gamma^3);$$

i.e., it has a quadratic tangency with the plane $\rho = 0$ along the line $\gamma = 0$. Furthermore, the fold point is located at

$$y = \Psi(\nu, \gamma, \bar{\lambda}) = -\frac{1}{\xi^0}\gamma + O(\gamma^2).$$

Since the fold bifurcation of pseudoequilibria must take place inside the sliding set Σ_s, we consider the expression $(\mathcal{L}_X f)(\mathcal{L}_Y f)$ which must be negative at $y = \Psi(\nu, \gamma, \bar{\lambda})$. Substituting $R(\nu, \gamma, \bar{\lambda})$ and $\Psi(\nu, \gamma, \bar{\lambda})$ for ρ and y, respectively, in $(\mathcal{L}_X f)(\mathcal{L}_Y f)$ we obtain a function $k(\nu, \gamma, \bar{\lambda})$ which must be negative when the PEF takes place in Σ_s. We find that

$$k(\nu, \gamma, \bar{\lambda}) = \frac{1}{\sigma\xi^0}\gamma + O(\gamma^2).$$

Thus for $\tau = \operatorname{sgn}\xi^0 = 1$ only the $\sigma\gamma \leq 0$ branch of $\mathcal{B}_{\mathrm{PEF}}$ is of interest while for $\tau = \operatorname{sgn}\xi^0 = -1$ only the $\sigma\gamma \geq 0$ branch is kept. ∎

4.2. Further simplification of bifurcation sets. In this section we show that the bifurcation diagram of any HT system satisfying the assumptions of Theorems 3.2 and 4.1 can be brought into one of eight standard forms depending on the value ± 1 of the parameters κ, σ, and $\tau = \operatorname{sgn}(\xi)$ with a smooth reparameterization. Furthermore, we describe in detail these standard forms.

Theorem 4.3 (bifurcation diagrams). *For the system* (3.1) *a diffeomorphism* $\varphi : (\tilde{\rho}, \tilde{\nu}, \tilde{\gamma}, \bar{\lambda}) \to (\rho, \nu, \gamma, \bar{\lambda})$ *exists on a small neighborhood of the origin in parameter space that sends the bifurcation set described in Theorem* 4.1 *to the bifurcation diagram that consists of the following sets expressed in new parameters* $(\tilde{\rho}, \tilde{\nu}, \tilde{\gamma})$:

(i) *Hopf bifurcation set* $\tilde{\nu} = 0$ *for* $\tilde{\rho} \geq 0$;
(ii) *grazing bifurcation set at* $\tilde{\nu} = -\kappa\tilde{\rho}^2$ *for* $\tilde{\rho} \geq 0$ *(cycle transition for* $\kappa\sigma = 1$, *cycle fold for* $\kappa\sigma = -1$);
(iii) *PEF bifurcation set at* $\tilde{\rho} = 1/(2\sigma\tau)\tilde{\gamma}^2$ *for* $\sigma\tau\tilde{\gamma} \leq 0$;
(iv) *ET set at* $\tilde{\rho} = 0, \tilde{\gamma} > 0$;
(v) *NSF bifurcation set at* $\tilde{\rho} = 0, \tilde{\gamma} < 0$.

Proof of Theorem 4.3. Observe that the Hopf, ET, and NSF bifurcation subsets of the system Z are already given in Theorem 4.1 in the form that is required here. Therefore, in order to construct the required reparameterizing diffeomorphism φ we need to kill the higher order terms in the description of the grazing bifurcation sets and the PEF bifurcation set.

Write the asymptotic expressions for the grazing bifurcation set in Theorem 4.1 as

$$\nu = -\kappa\rho^2 + O(\rho^3) = -\kappa\rho^2(1 + \rho\, n_1(\rho, \gamma, \bar{\lambda})),$$

where $n_1(\nu, \gamma, \bar{\lambda})$ is smooth in its arguments. For the PEF bifurcation set similarly write

$$\rho = \frac{1}{2\sigma\xi^0(\nu, \bar{\lambda})}\frac{\gamma^2}{1+\nu^2} + O(\gamma^3) = \frac{1}{2\sigma\tau}\gamma^2[r_0(\nu, \bar{\lambda}) + \gamma\, r_1(\nu, \gamma, \bar{\lambda})],$$

where

$$r_0(\nu, \bar{\lambda}) = \frac{1}{(1+\nu^2)|\xi^0(\nu, \bar{\lambda})|},$$

and $r_1(\nu, \gamma, \bar{\lambda})$ is smooth in its arguments. Note that $r_0(0, \bar{\lambda}) = |\xi(0, 0, 0, \bar{\lambda})|^{-1} \neq 0$.

Define the transformation $\varphi : (\tilde{\rho}, \nu, \tilde{\gamma}, \bar{\lambda}) \mapsto (\rho, \nu, \gamma, \bar{\lambda})$ given by

$$\tilde{\rho} = \rho \, [1 + \rho \, n_1(\rho, \gamma, \bar{\lambda})]^{1/2}, \quad \tilde{\gamma} = \gamma \, [r_0(\nu, \bar{\lambda}) + \gamma \, r_1(\nu, \gamma, \bar{\lambda})]^{1/2} [1 + \rho \, n_1(\rho, \gamma, \bar{\lambda})]^{1/4}.$$

The map φ sends the bifurcation diagram of Z to that described in the present theorem. Evaluating the derivative of the transformation at $\rho = \nu = \gamma = 0$ we find that the value of its determinant is

$$\det D\varphi(0, \bar{\lambda}) = [r_0(0, \bar{\lambda})]^{1/2} = |\xi(0, 0, 0, \bar{\lambda})|^{-1/2} \neq 0.$$

Therefore φ is a diffeomorphism in an open neighborhood of $\rho = \nu = \gamma = 0$. ∎

5. Dynamics of the truncated normal form. In this section we describe the dynamics of the truncated formal normal form Z in (3.1). In particular, we consider the system

(5.1a)
$$Z_0(x, y, \rho, \nu, \gamma) = \begin{cases} X_0(x, y, \nu) & \text{for } f_0(x, y, \nu) < \rho, \\ Y_0(x, y, \nu, \gamma) & \text{for } f_0(x, y, \nu) > \rho, \end{cases}$$

with

(5.1b)
$$X_0(x, y, \nu) = \begin{pmatrix} \nu & -1 \\ 1 & \nu \end{pmatrix} \begin{pmatrix} x \\ y \end{pmatrix} + \kappa(x^2 + y^2) \begin{pmatrix} x \\ y \end{pmatrix}$$

and

(5.1c)
$$Y_0(x, y, \nu, \gamma) = \begin{pmatrix} \sigma \\ \gamma - \sigma\nu + \frac{1}{2}\xi y \end{pmatrix},$$

where $f(x, y, \rho) = x - \rho$ and ξ is constant; cf. the full normal form in (3.1).

Note that for the vertical component of Y_0, which we denote by $Y_{0,2}$, truncating the formal normal form Y at linear terms would give

$$Y_{0,2} = \gamma - \sigma\nu + a_1(\lambda)x + a_2(\lambda)y,$$

instead of the form in (5.1c). Since we consider a straight boundary, we have $\xi = 2a_2(0)$. Furthermore, we ignore higher order terms in $a_2(\lambda) = a_2(0) + O(\lambda)$ since, for λ small enough, they do not induce any bifurcations of Y or in the sliding vector field Z_s. The term $a_1(\lambda)x$ is similarly omitted since it does not affect the bifurcations as determined in Theorem 4.1.

We now describe in detail the phase portraits of Z_0 for the four cases of bifurcation diagrams with $\kappa = -1$ discussed in the previous section and shown in Figure 5. As a further motivation for restricting only to the case $\kappa = -1$, note that Z_0 is invariant under the discrete transformation

$$\mathcal{R}' : (\kappa, \sigma, \xi; \rho, \nu, \gamma; x, y, t) \mapsto (-\kappa, -\sigma, -\xi; \rho, -\nu, \gamma; x, -y, -t),$$

which in parameter space corresponds exactly to the symmetry of the bifurcation diagram discussed in the previous section. For this reason for the study of the the dynamics of Z_0 it is enough to consider only the case $\kappa = -1$ and distinguish the four cases determined by the value of $\sigma = \pm 1$ and $\tau = \text{sgn}(\xi) = \pm 1$.

5.1. Case A1: $\kappa = -1$, $\sigma = -1$, $\tau = -1$. In this case the codimension-1 bifurcation sets separate the parameter space into seven open connected sets. Recall that since $\kappa = -1$, we have that $\nu_G = \rho^2 + O(\rho^3)$ for $\rho \geq 0$ determines the grazing bifurcation set $\mathcal{B}_G$. Furthermore, recall that the PEF set is given by $\mathcal{B}_{PEF} = \{\rho = (2\sigma\xi)^{-1}\mu^2 + O((\nu,\mu)^3),\ \mu \leq 0\}$, where we have taken into account that $\sigma\xi > 0$. Solving the defining equation of $\mathcal{B}_{PEF}$ for μ we obtain for $\rho \geq 0$ the solution μ_{PEF} that depends on ρ and ν and is, to the lowest order, $(2\sigma\xi\rho)^{1/2}$. With these definitions for ν_G and μ_{PEF} we denote the seven regions of the bifurcation diagram as follows:

I. $\rho < 0$
II. $\rho > 0$, $\mu < \mu_{PEF}$, $\nu < 0$
III. $\rho > 0$, $\mu < \mu_{PEF}$, $0 < \nu < \nu_G$
IV. $\rho > 0$, $\mu < \mu_{PEF}$, $\nu > \nu_G$
V. $\rho > 0$, $\mu > \mu_{PEF}$, $\nu < 0$
VI. $\rho > 0$, $\mu > \mu_{PEF}$, $0 < \nu < \nu_G$
VII. $\rho > 0$, $\mu > \mu_{PEF}$, $\nu > \nu_G$

The phase portraits for systems in each of these regions together with the transitions between them are shown in Figure 6. Passing from region II or IV to region I the system goes through an NSF bifurcation where a real equilibrium and a pseudoequilibrium collide and disappear. On the other hand, passing from region V or VII to region I the system goes through an ET where a real equilibrium gives its place to a pseudoequilibrium. In particular, in regions II, III, and IV the system has two pseudoequilibria, in region I it has one, and in regions V, VI, and VII it has no pseudoequilibria. Subsequently, the transitions II → V, III → VI, and IV → VII are PEF (saddle-node) bifurcations.

Passing from region II to III or from region V to VI the system goes through a Hopf bifurcation. The only difference between the two cases is related to the number of pseudoequilibria and not to the Hopf bifurcation itself. Finally, going from region III to IV or from region VI to VII we have a cycle transition grazing bifurcation.

5.2. Case A2: $\kappa = -1$, $\sigma = 1$, $\tau = 1$. This case has the same bifurcation diagram as case A1, so we adopt the same notation to refer to the seven regions. The phase portraits for systems in each of these regions together with the transitions between them are shown in Figure 7.

The types of bifurcations that we meet here are very similar to those in case A1. The main difference from case A1 is that the grazing bifurcation in this case is a cycle fold. Note that in regions III and VI a limit cycle coexists with a sliding cycle and when passing to regions IV and VII, respectively, these cycles collide and disappear.

5.3. Case B1: $\kappa = -1$, $\sigma = 1$, $\tau = -1$. In this case the codimension-1 bifurcation sets separate the parameter space into five open connected sets. We denote these regions as follows:

I. $\rho < 0$, $\mu < \mu_{PEF}$
II. $\rho < 0$, $\mu > \mu_{PEF}$
III. $\rho > 0$, $\nu < 0$
IV. $\rho > 0$, $0 < \nu < \nu_G$
V. $\rho > 0$, $\nu > \nu_G$
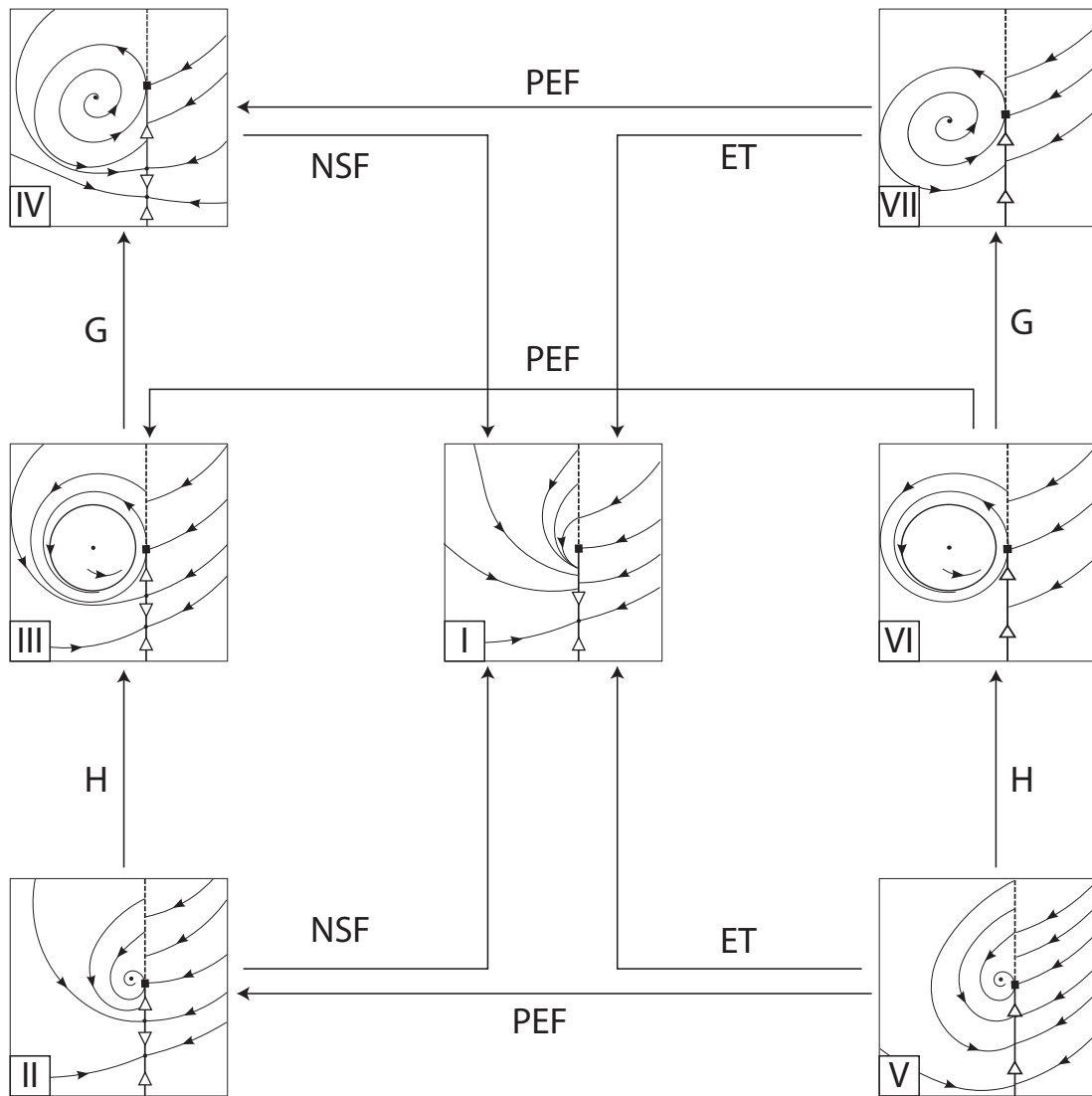
Figure 6. *Phase portraits corresponding to the open regions and codimension-1 bifurcations for case* A1.

Recall that since in this case we have $\sigma\xi < 0$, to lowest order it is $\mu_{\mathrm{PEF}} = (2\sigma\xi\rho)^{1/2}$ for $\rho \leq 0$. The phase portraits for systems in each of the five regions together with the transitions between them are shown in Figure 8. Passing from region III or V, where the system has one pseudoequilibrium and one real equilibrium, to region I, where there are no real or pseudoequilibria, we have an NSF bifurcation. Passing to region II, where there are two pseudoequilibria and no real equilibria, we find an ET. Regions I and II are consequently connected by a PEF. The transition III → IV is a Hopf bifurcation. Finally, going from region IV to V we have a cycle fold grazing bifurcation. Note that the sliding cycle in region IV is
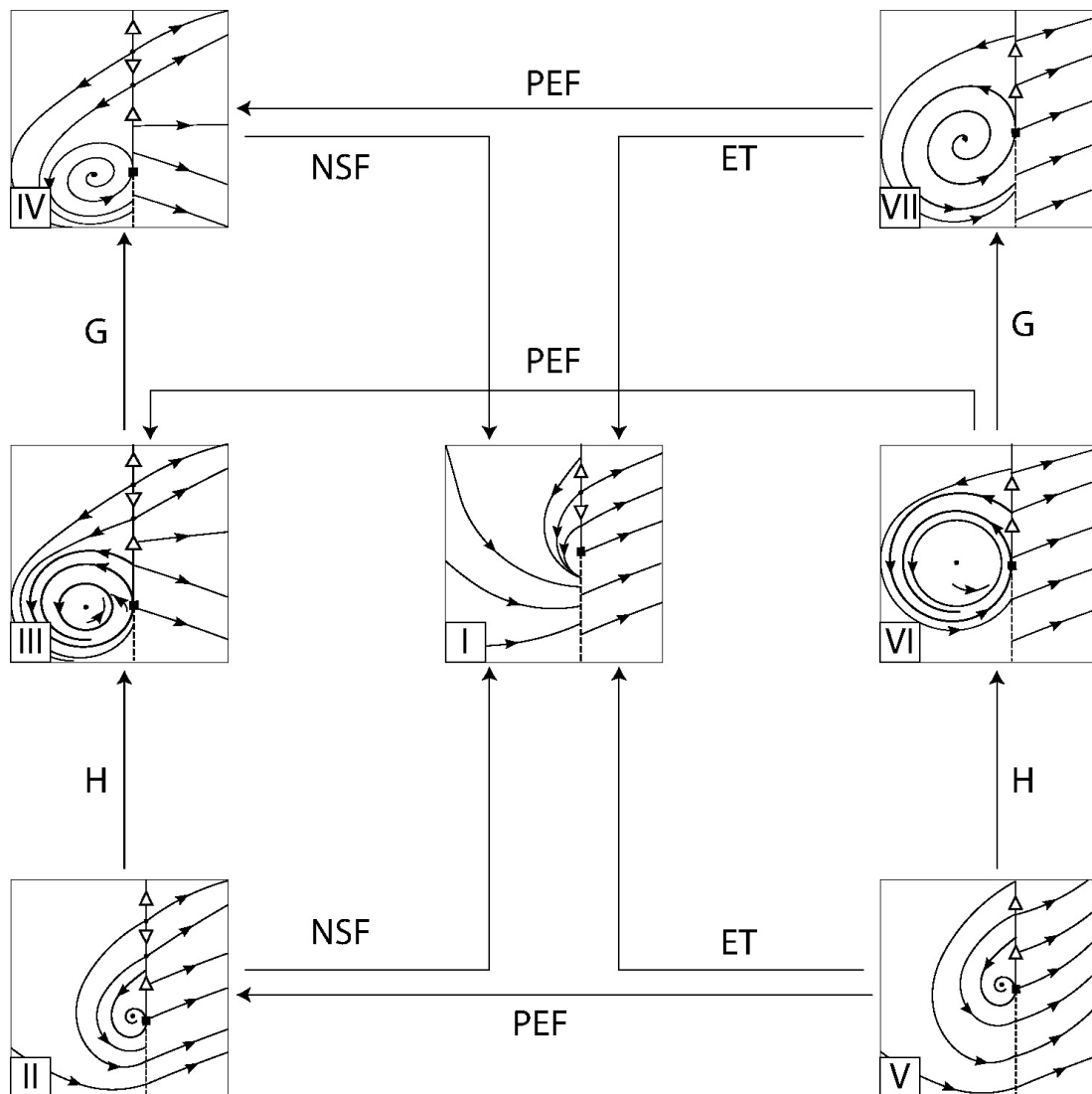
Figure 7. *Phase portraits corresponding to the open regions and codimension-1 bifurcations for case* A2.

a *reverse* sliding cycle, i.e., it becomes a sliding cycle if we follow the Filippov flow backward in time.

5.4. Case B2: $\kappa = -1$, $\sigma = -1$, $\tau = 1$. The bifurcation diagram is in this case very similar to that in case B1. The phase portraits for systems in each of the five regions together with the transitions between them are shown in Figure 9. The main difference between cases B2 and B1 is that in the present case the grazing bifurcation passing from region IV to V is a cycle transition.
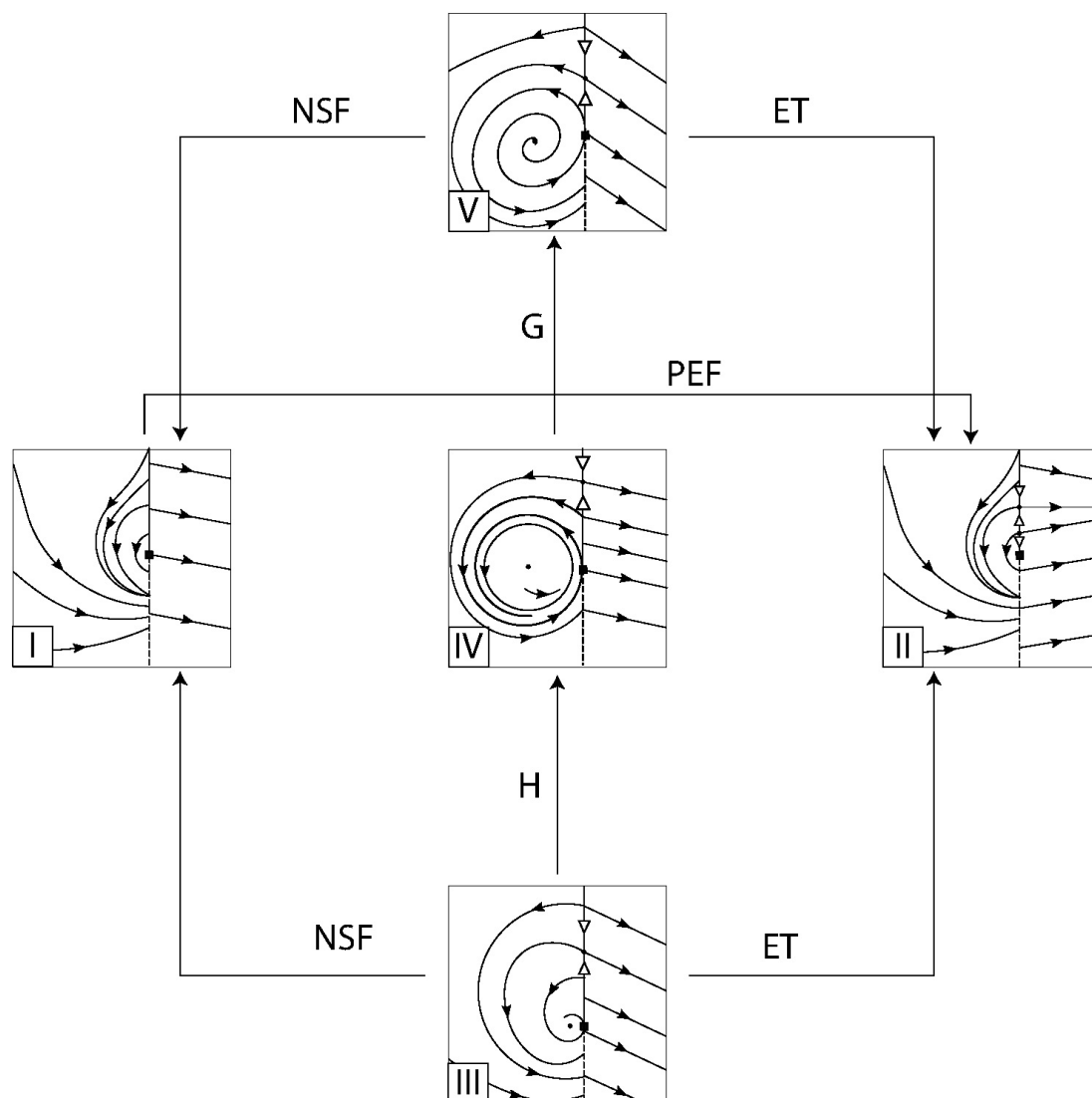
Figure 8. *Phase portraits corresponding to the open regions and codimension-1 bifurcations for case* B1.

6. An example from population dynamics.

As an example of an HT system that has a BHF point we consider a model from population dynamics. Different aspects of this model have been considered in [11, 24]. In [11], in particular, a parameter p is introduced in order to change the slope of the discontinuity boundary in such a way to avoid the degeneracy $\delta = 0$ associated to the BHF point. From this point of view the parameter p plays the role of the parameter $\gamma - \sigma\nu$ in the normal form of Theorem 3.2 that determines the slope of the vector field Y with respect to the discontinuity boundary.

In this population dynamics model there are two communities, a predator and a prey,
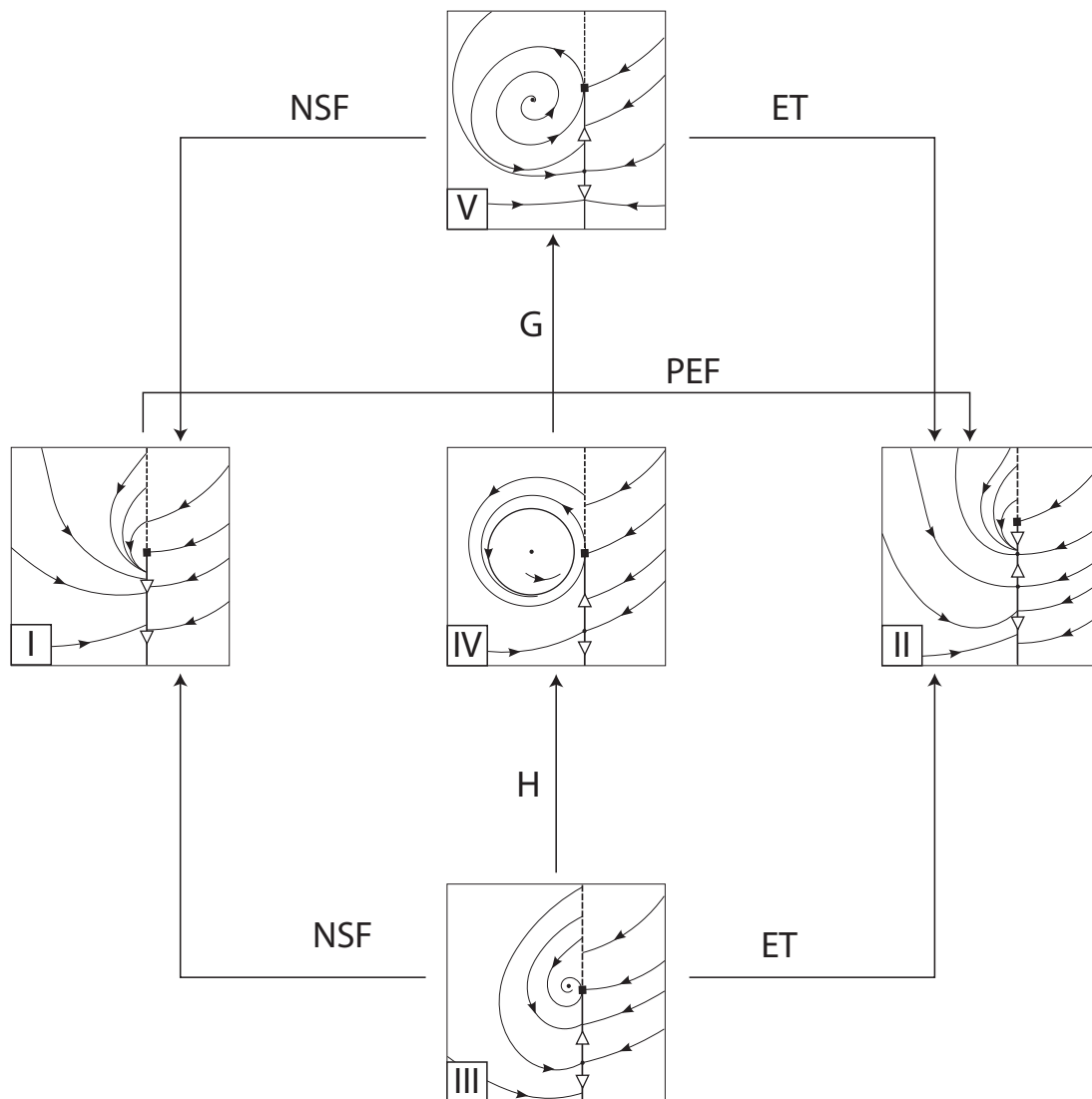
Figure 9. *Phase portraits corresponding to the open regions and codimension-1 bifurcations for case* B2.

with densities x and y, respectively. In the original model, when the prey density goes over a threshold r an extra harvesting term for the prey is introduced, proportional to the prey density. In the modified model, introduced in [11] and used here, the discontinuity boundary is given by the zero-set of

$$(6.1a) \qquad\qquad f(x, y; p, r) = x + py - r.$$

For $f(x, y; p, r) < 0$ the equations of motion are given by

$$(6.1\text{b}) \qquad X = \begin{pmatrix} \psi(y)x - dx \\ y(1-y) - \psi(y)x \end{pmatrix},$$

where

$$(6.1\text{c}) \qquad \psi(y) = \frac{ay}{b+y}.$$

Meanwhile, for $f(x, y; p, r) > 0$ we have

$$(6.1\text{d}) \qquad Y = \begin{pmatrix} \psi(y)x - dx - ex \\ y(1-y) - \psi(y)x \end{pmatrix} = X - \begin{pmatrix} ex \\ 0 \end{pmatrix}.$$

We assume that $a > d > 0$ and $e > 0$. For the numerical computations, following [11], we fix the parameter values $a = 0.3556$, $d = 0.04444$, $e = 0.2067$. Then the vector field X has a 1-parameter family of equilibria given by

$$x_0 = \frac{b}{a-d}\left(1 - \frac{db}{a-d}\right) = b\,(3.21378 - 0.458993\,b), \quad y_0 = \frac{db}{a-d} = 0.14282b.$$

This family goes through a Hopf bifurcation at

$$b_0 = \frac{a-d}{a+d} = 0.777822.$$

In particular, the eigenvalues of DX are equal to

$$\alpha \pm \mathrm{i}\,\omega \simeq -\frac{d}{2ab_0}(b - b_0) \pm \mathrm{i}\left[\omega_0 - \frac{d^2}{2a\omega_0}(b - b_0)\right]$$
$$= -0.080334(b - b_0) \pm \mathrm{i}\,[0.185920 - 0.014935(b - b_0)],$$

where the expression for the real part is exact (up to the precise value of the numerical coefficient) while the expression for the imaginary part is given up to first order terms in $b - b_0$. Here

$$\omega_0 = \omega(b_0) = \left(\frac{d(a-d)}{a+d}\right)^{1/2} = (db_0)^{1/2}.$$

We now verify that the conditions of having a BHF point in Definition 3.1 are satisfied for the point (x_0, y_0) at the parameter values

$$b = b_0, \quad p = p_0 = 0, \quad r = r_0 = x_0(b_0) = \frac{a}{(a+d)^2} = 2.22206.$$

Denoting by $\mu = (b, p, r)$ the system parameters we first find that

$$\nabla_{(x,y)} f(x_0, y_0; \mu_0) = (1, 0) \neq 0.$$

Then define $g(\mu) = x_0(b) + py_0(b) - r$ giving

$$\nabla_\mu g(\mu_0) = \left(\frac{1}{a+d}, \frac{d}{a+d}, -1 \right) = (2.49975,\ 0.111089,\ -1) \neq 0.$$

Therefore, condition (i) of Definition 3.1 is satisfied. For condition (ii) we have already seen that $\alpha(b_0) = 0$ and $\omega(b_0) = 0.185920 \neq 0$. Furthermore,

$$\nabla_\mu \alpha(\mu_0) = \left(-\frac{d(a+d)}{2a(a-d)},\ 0,\ 0 \right) = (-0.080334,\ 0,\ 0) \neq 0.$$

The value of the first Lyapunov coefficient is determined during the normalization of the vector field X. We find that

$$\ell_1(\mu_0) = -\frac{(a+d)d^2}{4a\omega_0^3} = -0.0864268 < 0,$$

and therefore X goes through a *supercritical* Hopf bifurcation so that in the normal form we will have $\kappa = -1$.

For condition (iii) we compute that

$$\mathcal{L}_Y f(x_0, y_0; \mu_0) = -\frac{ae}{(a+d)^2} = -0.459299 < 0.$$

This also shows that in the normal form we will have that $\sigma = -1$. For condition (iv) we find that the expression for δ for this system, evaluated at the equilibrium, is

$$\delta = \frac{eb(a+d)}{(a-d)^3} \left(b - b_0 - \frac{a(a-d)}{a+d} p \right) = 2.74469b(b - b_0 - 0.276594p).$$

Therefore, for $b = b_0$ and $p = 0$ we find that $\delta = 0$. Furthermore,

$$\nabla_\mu \delta(\mu_0) = \left(\frac{e}{(a-d)^2},\ -\frac{ae}{a^2 - d^2},\ 0 \right) = (2.13488,\ -0.590493,\ 0) \neq 0.$$

Finally, for condition (v) we can see from the expressions for $\nabla_\mu g(\mu_0)$, $\nabla_\mu \alpha(\mu_0)$, and $\nabla_\mu \delta(\mu_0)$ that they are linearly independent.

It follows that all conditions of Definition 3.1 are satisfied, and therefore Theorem 3.2 can be applied in order to bring the system into normal form. Nevertheless, we still have to check the condition of Theorem 4.1 concerning the bifurcation diagram, namely check the sign of ξ. In order to do this we need to bring the system in (6.1) into normal form by retracing the steps in the proof of Theorem 3.2.

Finally, we compute that

$$a_2(0) = \frac{e(a^2 - d^2 - 2d)}{3(a-d)[d(a^2 - d^2)]^{1/2}} = 0.105977$$

and

$$f_{yy}(0) = -\frac{4(a^2 - d^2 + d)}{3a^{1/2}[d(a^2 - d^2)]^{1/4}} = -1.38489$$
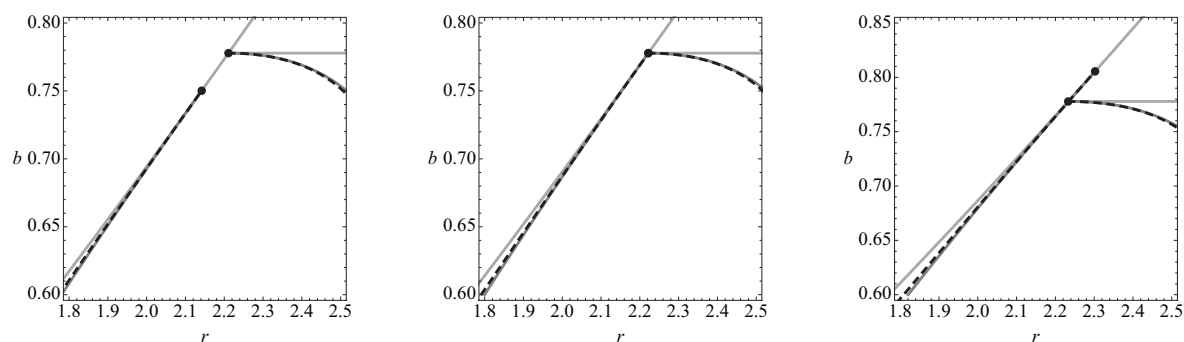
Figure 10. *Bifurcation diagrams near the BHF bifurcation point. (a) $p = -0.1$, (b) $p = 0$, (c) $p = 0.1$. The solid lines represent numerically computed bifurcation curves while the dashed lines represent the theoretically predicted bifurcation curves for the grazing bifurcation and the PEF bifurcation. Note the excellent match between numerically computed and theoretically predicted bifurcation curves.*

so that

$$\xi = 2a_2(0) + f_{yy}(0) = -1.17293 < 0.$$

This implies that this system is of type A1. Furthermore, the previous analysis shows that ξ changes sign, and therefore the system changes type from A1 to B2, when e increases above the critical value

$$e_c = \frac{2(a-d)(a^2 - d^2 + d)[d(a^2 - d^2)]^{1/4}}{a^{1/2}(a^2 - d^2 - 2d)} = 1.35056,$$

provided that the values of a and d are kept constant.

In Figure 10 we show the bifurcation diagram of the system close to the point (r_0, b_0) in the parameter subspace (r, b) where p is fixed and we consider three cases $p = 0, \pm 0.1$. The codimension-1 surface containing the ET and NSF bifurcations and the codimension-2 BH and BF points is given by

$$r = R(b, p) = x_0(b) + py_0(b).$$

More precisely, the codimension-2 BH family is parameterized by p as

$$r_{\mathrm{BH}} = R(b_0, p) = x_0(b_0) + py_0(b_0), \quad b_{\mathrm{BH}} = b_0.$$

The codimension-2 BF family is parameterized by p as

$$r_{\mathrm{BF}} = R(b_0 + 0.276594p, p), \quad b_{\mathrm{BF}} = b_0 + 0.276594p.$$

In order to complete the bifurcation diagram we computed the bifurcation curves for the grazing bifurcation and the PEF bifurcation. We computed these in two ways. First, we numerically computed the bifurcation curves by directly checking the conditions for the occurrence of those bifurcations. Second, we used the reparameterization $(r, b, p) \mapsto (\rho, \nu, \gamma)$ and the theoretic asymptotic expressions of Theorem 4.1, namely

$$\nu = \rho^2, \quad \rho \geq 0,$$

for the grazing bifurcation and

$$\rho = -\frac{1}{2\xi}\gamma^2, \quad \gamma \leq 0,$$

for the PEF bifurcation. We plotted both numerical and theoretical curves in Figure 10, the former with solid curves and the latter with dashed curves. Because the agreement between the two curves is very good, only the dashed curves are for the most part visible in Figure 10.

Finally, we give the asymptotic expressions for the grazing bifurcation and the PEF bifurcation. For the grazing bifurcation we have

$$4.9995b_s + (6.65038 + 0.714031p)b_s^2 - (4.9995 + 0.285641p)b_s r_s + r_s^2 = 0,$$

where $r_s = r - r_{\mathrm{BH}}$ and $b_s = b - b_{\mathrm{BH}}$. For the PEF bifurcation we have

$$\begin{aligned}(-2.42016 + 0.551217p)b_s + (1 - 3.57883p)b_s^2 \\ + (0.968162 - 0.177484p)r_s + (-0.641676 + 1.35193p)b_s r_s = 0,\end{aligned}$$

where $r_s = r - r_{\mathrm{BF}}$ and $b_s = b - b_{\mathrm{BF}}$.

7. Conclusions and discussion. This paper considered the boundary-Hopf-fold (BHF) bifurcation. This is a codimension-3 bifurcation of Hopf-transversal (HT) Filippov systems. We derived a smooth formal normal form and gave a detailed description of its bifurcations and the phase portraits. Furthermore, we demonstrated the BHF bifurcation in an example from population dynamics. A further extension of the present work is the study of HT systems using regularization techniques and singular perturbation theory; cf. [7, 27].

In section 6 we analyzed in detail how the BHF bifurcation manifests in a well-studied predator-prey model. Our analytical calculations showed in particular that we expect to find the BHF bifurcation for a very wide range of choices for the parameters a, d, e of the system. The conditions of Theorem 4.1 ask that the vector field X go through a Hopf bifurcation, and at the same time that Y be transversal to the boundary, while imposing some rather mild nondegeneracy conditions. For this reason we expect that almost all Filippov systems where an equilibrium of one of the vector fields goes through a Hopf bifurcation while at the discontinuity boundary will also have a BHF point, provided that the slope of the other vector field can sufficiently vary.

A further interesting question is how the BHF bifurcation manifests in higher-dimensional systems. We believe that a reduction to the center manifold will show that the extra dimensions do not affect the bifurcations described in the present work. This is currently a work in progress.

REFERENCES

[1] G. BARTOLINI, F. PARODI, V.I. UTKIN, AND T. ZOLEZZI, *The simplex method for nonlinear sliding mode control*, Math. Probl. Eng., 4 (1999), pp. 461–487.

[2] J.J.B. Biemond, N. van de Wouw, and H. Nijmeijer, *Bifurcations of equilibrium sets in mechanical systems with dry friction*, Phys. D, 24 (2012), pp. 1882–1894.

[3] B. Blazejczyk-Okolewska, K. Czolczynski, T. Kapitaniak, and J. Wojewoda, *Chaotic Mechanics in Systems with Impacts and Friction*, World Sci. Ser. Nonlinear Sci. Ser. A Monogr. Treatises 36, World Scientific, River Edge, NJ, 1999.

[4] H.W. Broer, *Bifurcations of Singularities in Volume Preserving Vector Fields*, Ph.D. thesis, University of Groningen, Groningen, The Netherlands, 1979.

[5] H.W. Broer, *Normal forms in perturbation theory*, in Encyclopedia of Complexity and System Science, Springer-Verlag, New York, 2009, pp. 6310–6329.

[6] H.W. Broer, V. Naudot, R. Roussarie, and K. Saleh, *A predator-prey model with non-monotonic response function*, Regul. Chaotic Dyn., 11 (2006), pp. 155–165.

[7] C.A. Buzzi, P.R. da Silva, and M.A. Teixeira, *A singular approach to discontinuous vector fields on the plane*, J. Differential Equations, 231 (2006), pp. 633–655.

[8] F. Della Rossa and F. Dercole, *Generalized boundary equilibria in n-dimensional Filippov systems: The transition between persistence and nonsmooth-fold scenarios*, Phys. D, 241 (2012), pp. 1903–1910.

[9] F. Della Rossa and F. Dercole, *The transition from persistence to nonsmooth-fold scenarios in relay control system*, in Proceedings of the 18th IFAC World Congress, Milano, Italy, 2011.

[10] F. Dercole, F. Della Rossa, A. Colombo, and Y.A. Kuznetsov, *Codimension-two singularities on the stability boundary in 2D Filippov systems*, in Proceedings of the 18th IFAC World Congress, Milano, Italy, 2011.

[11] F. Dercole, F. Della Rossa, A. Colombo, and Y.A. Kuznetsov, *Two degenerate boundary equilibrium bifurcations in planar Filippov systems*, SIAM J. Appl. Dyn. Syst., 10 (2011), pp. 1525–1553.

[12] F. Dercole, A. Gragnani, and S. Rinaldi, *Sliding bifurcations in relay control systems: An application to natural resources management*, in Proceedings of the 15th IFAC World Congress, Barcelona, Spain, 2002.

[13] F. Dercole, A. Gragnani, and S. Rinaldi, *Bifurcation analysis of piecewise smooth ecological models*, Theor. Popul. Biol., 72 (2007), pp. 197–213.

[14] F. Dercole and Y.A. Kuznetsov, *SlideCont: An Auto97 driver for bifurcation analysis of Filippov systems*, ACM Trans. Math. Software, 31 (2005), pp. 95–119.

[15] M. Di Bernardo, C.J. Budd, A.R. Champneys, and P. Kowalczyk, *Piecewise-Smooth Dynamical Systems: Theory and Applications*, Appl. Math. Sci. 163, Springer-Verlag, London, 2008.

[16] M. Di Bernardo, D.J. Pagano, and E. Ponce, *Non-hyperbolic boundary equilibrium bifurcations in planar Filippov systems: A case study approach*, Internat. J. Bifur. Chaos Appl. Sci. Engrg., 5 (2008), pp. 1377–1392.

[17] M. Fečkan, *Bifurcations and Chaos in Discontinuous and Continuous Systems*, Nonlinear Phys. Sci., Higher Education Press, Beijing; Springer, Heidelberg, 2011.

[18] A.F. Filippov, *Differential Equations with Discontinuous Righthand Sides*, Kluwer Academic Publishers, Dordrecht, The Netherlands, 1988.

[19] P. Glendinning, P. Kowalczyk, and A.B. Nordmark, *Attractors near grazing-sliding bifurcations*, Nonlinearity, 25 (2012), pp. 1867–1885.

[20] J.-L. Gouze and T. Sari, *A class of piecewise linear differential equations arising in biological models*, Dyn. Syst., 17 (2002), pp. 299–319.

[21] M. Guardia, S.J. Hogan, and T.M. Seara, *An analytical approach to codimension-2 sliding bifurcations in the dry-friction oscillator*, SIAM J. Appl. Dyn. Syst., 9 (2010), pp. 769–798.

[22] M. Guardia, T.M. Seara, and M.A. Teixeira, *Generic bifurcations of low codimension of planar Filippov systems*, J. Differential Equations, 250 (2011), pp. 1967–2023.

[23] P. Kowalczyk and P.T. Piiroinen, *Two-parameter sliding bifurcations of periodic solutions in a dry-friction oscillator*, Phys. D, 237 (2008), pp. 1053–1073.

[24] Y.A. Kuznetsov, S. Rinaldi, and A. Gragnani, *One-parameter bifurcations in planar Filippov systems*, Internat. J. Bifur. Chaos Appl. Sci. Engrg., 13 (2003), pp. 2157–2188.

[25] R.I. Leine, *Bifurcations in Discontinuous Mechanical Systems of Filippov's Type*, Ph.D. thesis, TU Eindhoven, Eindhoven, The Netherlands, 2000.

[26] R.I. Leine and H. Nijmeijer, *Dynamics and Bifurcation of Non-smooth Mechanical Systems*, Lect. Notes Appl. Comput. Mech. 18, Springer-Verlag, Berlin, Heidelberg, New York, 2004.

[27] J. LLIBRE, P.R. DA SILVA, AND M.A. TEIXEIRA, *Study of singularities in nonsmooth dynamical systems via singular perturbation*, SIAM J. Appl. Dyn. Syst., 8 (2009), pp. 508–526.

[28] J.E. MARSDEN AND M. MCCRACKEN, *The Hopf Bifurcation and Its Applications*, Appl. Math. Sci. 19, Springer-Verlag, New York, 1976.

[29] F. TAKENS, *Unfoldings of certain singularities of vector fields*, J. Differential Equations, 14 (1973), pp. 476–493.

[30] V.I. UTKIN, *Sliding Modes in Control and Optimization*, Springer-Verlag, Berlin, 1992.

[31] V.I. UTKIN, *Sliding mode control design principles and applications to electric drives*, IEEE Trans. Ind. Electron., 40 (1993), pp. 23–36.

[32] V.A. YAKUBOVICH, G.A. LEONOV, AND A.KH. GELIG, *Stability of Stationary Sets in Control Systems with Discontinuous Nonlinearities*, Ser. Stab. Vib. Control Syst. Ser. B 14, World Scientific, River Edge, NJ, 2004.

[33] Z.T. ZHUSUBALIYEV AND E. MOSEKILDE, *Bifurcations and Chaos in Piecewise-Smooth Dynamical Systems*, World Sci. Ser. Nonlinear Sci. Ser. A Monogr. Treatises 44, World Scientific, River Edge, NJ, 2003.